PNNL-28437

Pacific Northwest
NATIONAL LABORATORY

Degradation and Failure Phenomena of Accident Tolerant Fuel Concepts

Chromium Coated Zirconium Alloy Cladding

January 2019

KG Geelhood
WG Luscher

U.S. DEPARTMENT OF ENERGY

PACIFIC NORTHWEST NATIONAL LABORATORY
operated by
BATTELLE
for the
UNITED STATES DEPARTMENT OF ENERGY
under Contract DE-AC05-76RL01830

Printed in the United States of America

Available to DOE and DOE contractors from the
Office of Scientific and Technical Information,
P.O. Box 62, Oak Ridge, TN 37831-0062;
ph: (865) 576-8401
fax: (865) 576-5728
email: reports@adonis.osti.gov

Available to the public from the National Technical Information Service
5301 Shawnee Rd., Alexandria, VA 22312
ph: (800) 553-NTIS (6847)
email: orders@ntis.gov <http://www.ntis.gov/about/form.aspx>
Online ordering: http://www.ntis.gov

This document was printed on recycled paper.
(8/2010)

PNNL-28437

Degradation and Failure Phenomena of Accident Tolerant Fuel Concepts

Chromium Coated Zirconium Alloy Cladding

KG Geelhood
WG Luscher

January 2019

Prepared for
the U.S. Department of Energy
under Contract DE-AC05-76RL01830

Pacific Northwest National Laboratory
Richland, Washington 99352

Abstract

The U.S Nuclear Regulatory Commission (NRC) is preparing for anticipated licensing applications and commercial use of accident tolerant fuel (ATF) in United States commercial power reactors. PNNL has been tasked with providing technical assistance to the NRC related to the proposed new fuel and cladding designs. This report focuses specifically on the chromium metal and chromium compound coatings being investigated for the outer surface of Zr-alloy cladding. This report provides current state of the industry information on material properties and fuel performance considerations for Cr-coated cladding concepts in operating reactor conditions and reactor design basis accident conditions. To support the agency's readiness efforts, this report will identify and discuss degradation and failure modes of Cr-coated cladding concepts including fuel performance characteristics of Cr-coated cladding that may not be addressed within existing regulatory documents.

This report will provide an overview of the coating concepts that are currently being developed both in the US and around the world. Next, an overview of various coating techniques will be described to provide background on each coating technique that could be used. A discussion of the Cr-Zr phase diagram will be provided to identify any phases that should be avoided. Changes to fuel performance safety analysis codes, methods, and design limits will be discussed in the context of Cr-coated Zr for both normal conditions and accident conditions. This section will also identify any potential new damage mechanisms that are unique to Cr-coated Zr. The discussion of these damage mechanisms will also include discussion of existing or potential new data that could be used to develop or confirm design limits and performance relative to these design limits. Finally, a discussion of the current out-of-pile and in-pile data will be provided with special consideration to availability or lack of data to support the damage mechanisms and performance considerations previously identified.

Acknowledgments

This work was funded by the U.S. Nuclear Regulatory Commission under contract NRC-HQ-25-14-D-0001.

Acronyms and Abbreviations

AOO	Anticipated Operational Occurrence
ARMOR	Abrasion Resistant More Oxidation Resistant
ASME	American Society of Mechanical Engineers
ATF	Accident Tolerant Fuel
ATR	Advanced Test Reactor
BWR	Boiling Water Reactor
CEA	French Alternative Energies and Atomic Energy Commission
CFR	Code of Federal Regulations
CHF	Critical Heat Flux
CRUD	Chalk River Unknown Deposit (generic term for deposits on fuel cladding)
CVD	Chemical Vapor Deposition
DBA	Design Basis Accident
DC	Direct Current
DNB	Departure from Nucleate Boiling
DNBR	Departure from Nucleate Boiling Ratio
D-gun	Detonation gun
EPRI	Electric Power Research Institute
DOE	U.S. Department of Energy
GNF	Global Nuclear Fuels
HFIR	High Flux Isotope Reactor
HVOF	High-Velocity Oxy-Fuel
IBAD	Ion-Beam Assisted Deposition
IFA	Instrumented Fuel Assembly
INL	Idaho National Laboratory
KAERI	Korean Atomic Energy Research Institute
LOCA	Loss-of-Coolant Accident
LTR	Licensing Topical Report
LTA	Lead Test Assembly
LWR	Light Water Reactor
MBE	Molecular Beam Epitaxy
MCPR	Margin to Critical Power Ratio
MIT	Massachusetts Institute of Technology
MITR	Massachusetts Institute of Technology Reactor
MOCVD	Metallo-Organic Chemical Vapor Deposition
NEA	Nuclear Energy Agency
NRC	U.S. Nuclear Regulatory Commission

NSRR	Japanese Test Reactor
OECD	Organization for Economic Cooperation and Development
ORNL	Oak Ridge National Laboratory
PNNL	Pacific Northwest National Laboratory
PTFE	Polytetrafluoroethylene
PVD	Physical Vapor Deposition
PWR	Pressurized Water Reactor
RF	Radio Frequency
RIA	Reactivity Initiated Accident
SAFDL	Specified Acceptable Fuel Design Limit
SRP	Standard Review Plan
Zry	Zircaloy
Zry-2	Zircaloy-2
Zry-4	Zircaloy-4

Contents

Figures

Tables

1.0 Introduction

The U.S Nuclear Regulatory Commission (NRC) is preparing for anticipated licensing applications and commercial use of accident tolerant fuel (ATF) in United States commercial power reactors. Several fuel vendors, in coordination with the Department of Energy (DOE), have announced plans to develop and seek approval for various fuel designs with enhanced accident tolerance (i.e., fuels with longer coping times during loss of cooling conditions). The designs being considered in the development of this plan include Cr coated claddings, Cr-doped UO_2 pellets, FeCrAl cladding, SiC cladding, U_3Si_2 pellets, and metallic fuels. These designs represent evolutions and deviations from the *de facto* standard zirconium alloy clad, uranium dioxide fuel form. Most of the NRC's regulatory framework was developed specifically for zirconium alloy clad, uranium dioxide fuel and is only applicable to this system.

PNNL has been tasked with providing technical assistance to the NRC related to the proposed new fuel and cladding designs. This report and others like it will provide the agency with expert technical assistance to enhance the staff's knowledge base of specific accident tolerant fuel concepts and will support the agency's efforts to develop and review the required regulatory infrastructure to support the development of accident tolerant fuel.

This report will provide current state of the industry information on material properties and fuel performance considerations for Cr-coated cladding concepts in operating reactor conditions and reactor design basis accident conditions. To support the agency's efforts, this report will identify and discuss degradation and failure modes of Cr-coated cladding concepts including fuel performance characteristics of Cr-coated cladding that may not be addressed within existing regulatory documents (e.g., 10 CFR, regulatory guidance, NUREG-0800).

The scope of this report includes metallic coatings of chromium that are in development for ATF cladding as well as any ceramic coatings that are being developed for ATF claddings. This entire class of concepts will be generically referred to as "Cr-coated Zr" throughout this report. This report will provide an overview of the coating concepts that are currently being developed both in the US and around the world (Section 2.0). Next an overview of various coating techniques will be described to provide background on each coating technique that could be used (Section 3.0). A discussion of the Cr-Zr phase diagram will be provided to identify any phases that should be avoided (Section 4.0). Changes to safety analysis codes, methods, and design limits will be discussed in the context of Cr-coated Zr for both normal conditions and accident conditions (Section 5.0). This section will also identify any potential new damage mechanisms that are unique to Cr-coated Zr. The discussion of these damage mechanisms will also include discussion of existing or potential new data that could be used to develop or confirm design limits and performance relative to these design limits. Finally, a discussion of the current out-of-pile and in-pile data will be provided (Section 6.0) with special consideration to availability or lack of data to support the damage mechanisms and performance considerations previously identified.

1.1 Background

The 2011 Great East Japan Earthquake and Tsunami, and the events that followed at the Fukushima Daiichi power plant led to a worldwide interest in development of fuels with enhanced performance during such rare events. In response, accident tolerant fuel development programs were started in many research institutions and industry teams. A new fuel system alone is insufficient to completely mitigate

accident consequences, however, a new fuel in combination with other systems may provide some margin in responding to such rare events, while providing additional benefits during more frequent events and/or normal operations.

For light-water reactors (LWRs) the cladding has historically been fabricated from zirconium alloys. For boiling water reactors (BWRs) the alloy Zircaloy-2 was used. For pressurized water reactors (PWRs) the alloy Zircaloy-4 has been used. As demand for higher burnup levels came for LWR fuels, in-reactor cladding corrosion became a problem. To reduce the in-reactor corrosion and maintain or improve the creep properties of the cladding, the nuclear fuel vendors have developed proprietary, Zr-based cladding alloys that have mostly replaced the use of traditional Zircaloy alloys. Westinghouse now uses the alloys, ZIRLO and Optimized ZIRLO for their PWR fuel, while retaining Zircaloy-2 for BWR fuel. Framatome uses M5® for their PWR fuel, while also retaining Zircaloy-2 for BWR fuel. Global Nuclear Fuels (GNF) only supplies BWR fuel and has recently received approval for ZIRON cladding.

Although accident tolerant fuel cladding is being developed primarily to give an advantage during high temperature oxidation that may occur following an accident, there are a general set of requirements that are placed on nuclear fuel cladding. These requirements are that the cladding retain shape, retain all pellets and fission products, and effectively transfer heat to coolant with a surface flux of about 600,000 W/m^2.

The specific damage and failure mechanisms that have historically been identified for LWR fuel are discussed in greater detail in Section 5.2. In general, safety analysis is performed prior to operation to show:

- Rods will not fail during normal operation and anticipated operational occurrences (AOOs)
- Rods may fail during a design basis accident. If rods fail during a design basis accident, the number of failed rods should not be underestimated for dose considerations and failure should not result in a loss of coolable geometry.

The reactor conditions that LWR cladding are exposed to under normal operations are as follows:

Boiling Water Reactor (BWR)

- Liquid water from 530°F (277°C) to 550°F (288°C) at 1035 psi (7.1 MPa) and steam at 550°F (288°C) and 1035 psi (7.1 MPa)
- Coolant mass flux of 1.05×10^6 lb/ft²-hr (1427 kg/m²-s)
- Fast neutron flux 1×10^{18} n/m²-s
- Time in core of 1500 to 2000 days.
- Rod-average burnup of 62 GWd/MTU

Pressurized Water Reactor (PWR)

- Liquid water 550°F (288°C) to 610°F (321°C) at 2250 psi (15.5 MPa)

- Coolant mass flux of 2.55×10^6 lb/ft²-hr (3466 kg/m²-s)
- Fast neutron flux 1×10^{18} n/m²-s
- Time in core of 1500 to 2000 days.
- Rod-average burnup of 62 GWd/MTU

The cladding conditions during anticipated operational occurrences are not significantly different than those during normal operation and typically result in brief changes in power or coolant flow rate. These changes are less than 50% of the nominal values.

As mentioned before, design basis accidents have been identified for LWRs and during these events failure of the cladding is permitted, but the number of failed rods should not be underestimated, and the failure of rods should not impact the coolability of the fuel assembly. The main design basis accidents of interest to the fuel design review are: reactivity initiated accident (RIA) and loss-of-coolant accident (LOCA). The conditions and fuel damage anticipated are described below.

Reactivity Initiated Accident (RIA)

This accident is caused by a rapid removal of a control rod or control blade from the core that results in an extreme increase in power in nearby fuel rods (1000 times increase) over a very short time (~20 ms) that then goes back to zero power. This event results in thermal expansion of pellet which can contact the cladding and causes relatively large (1-5%) hoop strain in the cladding at relatively low temperature (<700°C). This pellet-clad mechanical interaction can cause cladding failure and, if extreme enough, can lead to violent expulsion of the fuel from the cladding which can result in a loss of coolable geometry or a pressure pulse that can damage the reactor vessel.

Loss-Of-Coolant Accident (LOCA)

This accident is a significant loss of coolant in the core. In the case of a large pipe break, the accident can involve rapid depressurization of the reactor core and complete loss of water to the core. In the case of a small pipe break, the accident may be characterized by a slower depressurization and partial loss of water to the core. Although the fission process is stopped by automatic control rod insertion, this loss of active cooling leads to heating of fuel rod from decay heat. Ballooning and burst of fuel rods are observed between 800-1000°C and high temperature oxidation of cladding with steam, an exothermic reaction which creates additional heat, is observed between 1000°C and 1200°C. At some point during the event, the emergency core cooling system will reflood the reactor with water, resulting in potential rapid cooling of the fuel rods by water quench. Numerous mechanisms for fuel cladding failure exist in the accident, including ballooning and burst where fuel may be ejected from the fuel rods and high temperature corrosion could embrittle the cladding leading to fuel fracture and a loss of coolable geometry during the reflood phase.

The Fukushima accident would be considered a beyond design basis accident. In this event there was a long-term loss of offsite power and no onsite generating capacity, leading to an inability to remove decay heat from the shut-down reactor core. After an extended period, the water in the core boiled off and the cladding reacted with the steam to produce hydrogen. The hydrogen was insufficiently vented from the

reactor building and after a critical concentration of hydrogen accumulated it caused an explosion. Currently the U.S. has no regulations related to fuel performance and qualification during events and accidents classified as "beyond design basis.[1]" However, work is currently being done with the goal of improving the performance of the fuel assemblies at temperatures above 1200°C (Brachet, et al., 2018) (Oelrick, Xu, Lahoda, & Deck, 2018) which would currently represent performance beyond design basis.

1.2 Previous Reviews

Three publications have been identified as providing a reasonable overview of the work that has been done to support the development of accident tolerant fuels. Oak Ridge National Laboratory (ORNL) published a review paper in the Journal of Nuclear Materials summarizing the status and challenges associated with accident tolerant fuel (Terrani, 2018). The Organization for Economic Cooperation and Development – Nuclear Energy Agency (OECD-NEA) has published a state-of-the-art report on light water reactor accident tolerant fuels (OECD, NEA, 2018). Finally, the Electric Power Research Institute (EPRI) has published a gap analysis on coated cladding being developed for accident tolerant fuels (Csontos, 2018). The rest of this section briefly describes each of these reports.

OECD-NEA Report

The OECD-NEA state-of-the-art report discusses the work being done on all ATF concepts. Chapter 10 of that report describes the coated cladding concepts. This report discusses some development and data collection activities that have been performed. The most useful information from this report is a summary of the main advantages of coated cladding and the challenges to be monitored. These are as follows, taken directly from (OECD, NEA, 2018).

Main advantages:

- low neutronic penalty if coating is sufficiently thin (<20 μm);
- similar mechanical behaviour as uncoated cladding if coating is sufficiently thin (<20 μm);
- significant reduction in corrosion kinetics for metallic coatings (Cr, Cr-Al, FeCrAl) and for some ceramic coatings (CrN and TiN) → increased margins and longer exposure times expected;
- significantly reduced hydrogen pickup and therefore hydrogen embrittlement for these same coatings → increased margins and longer exposure times expected;
- increased wear resistance → reduced fuel rod failures due to fretting are expected (but needs further assessment in representative irradiation conditions up to high burn-up).

Challenges to be monitored:

- coating thickness;
- dissolution of Al-containing coatings (TiAlN, CrAlN, and to a significantly lower extent FeCrAl);
- irradiation impact on coatings, which may lead to cracks or local removal of the coating;
- lack of out-of-pile data on the mechanical behaviour of ceramic coatings;
- lack of in-pile mechanical behaviour data in representative LWR conditions, especially at high burn-up;

[1] Note that NRC has various requirements for beyond design basis accidents, including the station blackout rule (10 CFR 50.63), the anticipated transient without scram rule (10 CFR 50.62), and requirements for maintaining or restoring core and spent fuel pool cooling and containment integrity in the event of large explosions or fires (10 CFR 50.54 (hh)(2), also known as B.5.b). NRC has also published a proposed rule (SECY-15-0065) governing various aspects of beyond design basis accidents that originated as part of the post-Fukushima lessons learned activities. However, none of these rules and regulations establish specific requirements for fuel performance or qualification for beyond design basis accidents.

- lack of out-of-pile corrosion behaviour of MAX phase coatings in normal operating conditions.

PNNL staff generally agree with these conclusions, however this report will produce its own conclusions regarding lack of data and challenges.

Review Article in *Journal of Nuclear Materials*

The review article in *Journal of Nuclear Materials* also discusses the work being done on all ATF concepts. This article reviews coatings of Cr, CrN, CrAlN, TiAlN, TiN/TiAlN, Ti_2AlC, Ti_3SiC_2, and CrAlC. In general, it was concluded that in terms of corrosion resistance and neutron stability, the Cr and CrN are the most promising. In the case of Cr-coating and CrN-coatings, it concludes that both coatings are resistant to corrosion in LWR coolant and stable under neutron irradiation at expected temperatures. It concludes that Cr-coatings provide increased resistance to high temperature steam oxidation while CrN does not. The scope of these conclusions only assists in determining if a concept should even be evaluated for ATF research and do not discuss the requirements for licensing of such fuel as this current report has.

EPRI Gap Analysis Report

The EPRI Gap analysis attempts to identify gaps related to the licensing of Cr-coated cladding. To do this, the report identifies gaps in three general areas; 1) fuel performance phenomena and modeling gaps, 2) material and behavior model gaps, and 3) technical licensing/regulatory gap analysis. The following gaps were identified in each area.

<u>Fuel performance phenomena and modeling gaps</u>

- Simulation meshing capabilities
- Material interfaces
- Material model implementation
- Validation of the computer code
- Problem initialization.

<u>Material and behavior model gaps</u>

- Material properties (thermal)
- Material properties (mechanical)
- Diffusion of Cr coating into Zr substrate
- Cracking and/or delamination of coating.

<u>Technical licensing/regulatory gaps</u>

- Damage at the substrate/coating interface related to microcracking, localized embrittlement and system effects
- Fretting damage to grid components from hard coatings on cladding

- CRUD deposition affecting heat transfer during AOOs and DBAs
- Coating spallation leading to coolability issues with pump screen clogging.

These gaps, as well as additional gaps that have been identified, will be discussed throughout this report.

Regarding the gaps identified above, PNNL agrees that validation of the computer code and material model implementation remain as gaps and detailed information regarding validation of the computer code is provided in this report. Depending on an applicant's approach, the simulation meshing capabilities, material interfaces, and problem initialization may not be necessary (see Section 5.0). PNNL agrees with the material property needs and has provided discussion on specific material property needs (see Section 5.1). Diffusion of coating into cladding, cracking of the coating, and delamination of the coating are all new damage mechanisms discussed in this report (see Section 5.2.4) as well as radiation effects on Cr (Not identified in the EPRI report). The EPRI identified technical/regulatory gaps are all discussed in Section 5.2 as well as several others. While an important consideration for operation, the CRUD deposition issue does not seem particularly relevant to licensing. As with Zr-alloy cladding, the CRUD should be monitored in plants and should be explicitly considered if it is present and modeled as an insulating layer around the fuel rod.

2.0 Overview of Coating Concepts

This section provides an overview of coating concepts that are currently being developed for ATF cladding. Special focus is provided to those concepts being developed by U.S. fuel manufacturers (Sections 2.1 to 2.3). Table 2.1 provides a high-level overview of the U.S. Cr-coated cladding concepts. Information is also provided on those concepts being developed outside the U.S. and by various research organizations. Although these particular concepts may not have a short-term path to U.S. licensing, the research and development being done on them may identify relevant degradation mechanisms or data that could be applied to those concepts that do have a near-term path to U.S. licensing.

Table 2.1 Comparison of Cr-Coated Concepts being Pursued by U.S. Nuclear Fuel Vendors

Vendor	Coating	Application Process	Coating Thickness
Westinghouse	Cr-coated ZIRLO®	Cold spray and polishing	20-30 μm
Framatome	Cr-coated M5®	PVD	8-22 μm
GNF	ARMOR coated Zircaloy-2	*proprietary*	*proprietary*

2.1 Westinghouse

Westinghouse is currently working toward commercializing two ATF designs. The first is silicon carbide (SiC) cladding with uranium silicide (U_3Si_2) fuel. The second is chromium-coated zirconium alloy cladding with U_3Si_2 fuel. Westinghouse refers to all their ATF fuel concepts as EnCore® fuel. In addition to U_3Si_2 fuel, Westinghouse is also working to commercialize their advanced doped UO_2 fuel (ADOPT™ fuel) with Cr-coated cladding (Oelrich, et al., 2018).

The Cr-coated cladding being developed by Westinghouse consists of ZIRLO® and Optimized ZIRLO™ cladding coated with chromium using a cold spray process. Application parameters for cold spray have been optimized to achieve dense and adherent coatings, while polishing processes have been developed to achieve the thickness and surface finish required for in-reactor performance and seamless integration into current fuel designs, without a need for fuel assembly structure modifications (Shah, et al., 2018). The final coating thickness is between 20 and 30 μm.

Westinghouse has performed ex-reactor testing on their Cr-coated cladding including:

- Corrosion in pressurized water
- High temperature corrosion in steam
- CRUD deposition
- Mechanical testing.

The effect of surface imperfections and scratches is currently being evaluated. Further details of the ex-reactor testing are provided in Section 6.0.

Westinghouse has performed in-reactor testing on Cr-coated cladding in the MIT reactor and the Halden reactor. Lead test rods of Cr-coated Zr with U_3Si_2 fuel and doped UO_2 fuel (ADOPT™ are planned for irradiation in the Byron reactor (3645 MWt PWR operated by Exelon Generation Co.) in Spring 2019. Current plans are for lead test assemblies (LTAs) of SiC and Cr-coated Zr with U_3Si_2 fuel and doped UO_2 fuel (ADOPT™) by 2022 and batch implementation by 2027 (Shah, et al., 2018). Further details of the in-reactor testing are provided in Section 6.0.

2.2 Framatome

Framatome is currently working toward commercializing a near-term ATF design. This design includes chromium-coated zirconium alloy cladding (M5®) with Cr_2O_3 doped UO_2 fuel (Bischoff, et al., 2018). In the long-term, Framatome is developing SiC/SiC composite cladding.

The Cr-coated cladding being developed by Framatome consists of M5® cladding coated with chromium using a physical vapor deposition process. The coating deposited is very dense and adherent. Additionally, the PVD technique that is used does not modify the underlying substrate microstructure since no heat treatment is applied on the tubes during deposition and the increase in temperature due to the incident Cr atoms is relatively small (Bischoff, et al., 2018). No additional processing steps following PVD deposition have been described by Framatome. The final coating thickness is between 8 and 22 μm.

Framatome has performed ex-reactor testing on their Cr-coated cladding including:

- High temperature corrosion in steam and quench
- Debris and component wear resistance in normal operation
- Ballooning behavior
- Mechanical tests
- Autoclave corrosion at 360°C.

Further details of the ex-reactor testing are provided in Section 6.0.

Framatome has performed in-reactor testing in Gösgen, Halden, and ATR. Lead test rods of Cr-coated Zr with Cr_2O_3 doped UO_2 fuel are planned for irradiation in the Vogtle reactor (3625 MWt PWR operated by Southern Nuclear Operating Co.) and the ANO-1 reactor (2568 MWt PWR operated by Entergy Operations) (Bischoff, et al., 2018) in early 2019. Further details of the in-reactor testing are provided in Section 6.0.

2.3 GNF

GNF is currently working toward commercializing of two near-term ATF designs. The first is IronClad (FeCrAl) cladding with UO_2 fuel. The second is Abrasion Resistant, More Oxidation Resistant (ARMOR) cladding (coated zirconium alloy cladding) with UO_2 fuel. (Lin, et al., 2018).

The coated cladding being developed by GNF consists of Zircaloy-2 cladding coated with a proprietary coating. The following parameters have not been documented in public references for ARMOR:

- Chemical composition of the coating
- Application process for the coating
- Thickness of the coating

GNF has performed ex-reactor testing on their ARMOR-coated cladding including:

- Wear resistance
- Corrosion under normal operational conditions
- High temperature corrosion in steam
- Thermal cycling.

Further details of the ex-reactor testing are provided in Section 6.0.

Lead test rods of ARMOR-coated Zr with UO_2 fuel are underway in the Hatch reactor (2804 MWt BWR operated by Southern Nuclear Operating Co.) since spring of 2018. Current plans for batch implementation of ARMOR coated rods is 2020 or 2021 (Lin, et al., 2018). Further details of the in-reactor testing are provided in Section 6.0.

2.4 Korea

The Korean Atomic Energy Research Institute (KAERI) has been investigating a number of different coatings and application techniques (Kim, et al., 2018) (Kim, Yang, Kim, & Koo, 2016). These include 3D laser coating of Cr and CrAl (Kim, et al., 2015) and cold spray of Cr (Park, et al., 2016). Research on both of these concepts includes:

- Adhesion
- Formation of a heat affected zone
- High temperature steam oxidation
- Tensile tests
- Ballooning and burst.

KAERI provided coated cladding samples that have been irradiated in IFA-796 (Szoke & Bennett, 2017). No other plans for irradiation tests on these concepts have been indicated.

2.5 China

Various Chinese state organizations are working on development of a number of different coated cladding concepts. These include Cr and CrN coating by PVD (Liu, et al., 2018) and plasma sprayed Cr coatings (Wang, et al., 2018). Research on both of these concepts includes:

- Oxidation at 1200°C
- Investigation of the coating/substrate interaction zone

- Autoclave corrosion.

Further details of the ex-reactor testing are provided in Section 6.0.

No plans for irradiation tests on these concepts have been indicated.

2.6 Other Research Groups

Other groups are doing independent research on coated cladding concepts. The full details of this research is provided in Section 6.0.

Halden Reactor irradiated test rods clad in Zr coated in CrN, AlCrN, and TiAlN in IFA-774 (Anderson & Van Nieuwenhove, 2016) (Van Nieuwenhove, 2014). Neither the TiAlN nor the AlCrN coating survived the test. The CrN coating performed better but displayed cracking and missing parts with about 80% of the coating remaining. Halden also irradiated test rods clad in Zr coated with Cr provided by Westinghouse and Framatome and Zr coated with CrAl provided by KAERI in IFA-796 (Szoke & Bennett, 2017). The reactor has been shut down before the planned burnup could be obtained. Post irradiation examination is underway.

Massachusetts Institute of Technology (MIT) and The Czech Technical University (CTU) have been investingating Zircaloy samples coated in Cr by cold spray and E110 coated with Cr and CrN by PVD (Sevecek, et al., 2018) (Sevecek, et al., 2018) (Shahin, Petrik, Seshadri, Phillips, & Shirvan, 2018) (Krejci, et al., 2018). Tests on these samples include:

- 500°C and 1200°C to 1500°C steam oxidation
- Overpressure tests
- Fatigue failure
- Burst test
- Corrosion in 360°C water
- Interdiffusion above eutectic 1333°C.

Further details of the ex-reactor testing are provided in Section 6.0.

3.0 Overview of Coating Techniques

Brief overviews for a wide array of coating techniques are provided in this section. While a detailed evaluation of each technique is outside the scope of this report, the intent here is to provide a high-level overview of selected techniques and discuss the general advantages and disadvantages. It is important to note that these coating techniques, like most manufacturing processes, have several parameters that can be tailored to accommodate various challenges in producing engineered coatings. Furthermore, the techniques themselves can be modified and, in some cases, combined, to produce the desired result. This results in numerous similar coating technologies that are within, and between, the general categories identified and discussed in the following sections. These categories include physical vapor deposition, chemical vapor deposition, electrodeposition, thermal spray, cold spray, and pack cementation.

3.1 Physical Vapor Deposition

Physical vapor deposition (PVD) is a broad term used to describe the deposition of atoms, molecules, or the combination of atoms and molecules via condensation. In general, the term PVD encompasses evaporation, sputtering, and ion plating processes. These three processes are described in the following subsections (Pierson, 1999) (Grainger, 1998).

3.1.1 Evaporation

Evaporative coatings are applied by heating the coating material (i.e., source) above the boiling point under low pressure ($<10^{-3}$Pa). This sends atoms or molecules through a cosine distribution of trajectories in a straight line to the substrate where they condense and form a thin film. At these low pressures, the mean-free path is large relative to the distance between the source and substrate and few collisions occur before the species condense on the substrate. This may lead to uneven coating thickness because the thickest part will be closest to the source. Uneven coatings may be avoided by employing planetary substrate holders and multiple sources. Evaporative coatings offer relatively high deposition rates (up to 75 μm/min) but complex shapes are difficult to accommodate, and the coatings often exhibit poor adhesion. A variety of different techniques are available for depositing evaporative coatings such as reactive evaporation, plasma assisted or activated reactive evaporation, and molecular beam epitaxy. These techniques are described briefly in this section (Pierson, 1999).

Reactive evaporation can be used to deposit refractory carbides, nitrides, and oxides, which have extremely high boiling points and tend to dissociate during evaporation. During reactive evaporation, the nonmetallic element of the coating (e.g. carbon, nitrogen, or oxygen) is introduced into the gas phase and a pure metal source is used (e.g. nitrogen used with a titanium source can produce titanium nitride) (Pierson, 1999).

Plasma assisted or reactive evaporation can be used to enhance depositions rates using a plasma. A plasma is an ionized gas that is formed in the presence of an electromagnetic field under vacuum. The presence of the plasma enhances reactions in the gas phases and the growth kinetics of the deposit (Pierson, 1999).

Molecular beam epitaxy (MBE) is another form of evaporative coating and can be used to produce extremely pure and very thin films with abrupt composition changes. The deposition rate for MBE is very slow and the process is still considered experimental. Nevertheless, MBE is considered for extremely exacting electronic and optoelectronic applications (Pierson, 1999).

3.1.2 Sputtering

Sputtering is a technique used to create thin films. It is extensively used in the hard coating industry. High quality coatings of refractory compounds and metals can be readily produced with good adhesion and composition control. In addition, since sputtering is not a thermally activated process, it is not associated with high temperature requirements like other coating processes (Pierson, 1999).

During the sputtering process, a source (or target) is placed in a high vacuum and bombarded with gas ions (typically argon) which have been accelerated by high voltage, producing a glow discharge or plasma. Atoms from the target are physically ejected by the momentum transfer and travel across the vacuum chamber and are deposited on a substrate surface. Since the process is performed under low pressure, the mean-free path of the target atoms is relatively long, thus permitting the ejected atoms to condense on the intended surface (Pierson, 1999).

Sputtering requires low pressure to remove all traces of background and contaminant gases which could degrade the coating. This is typically achieved by cryogenic pumps capable of producing a vacuum of about 10^{-5} Pa with good pumping speed. After evacuation, the system is refilled with argon to a partial pressure of 0.1 to 10 Pa. Higher pressure, by placing too many argon atoms in the path of the ions and ejected atoms, would not allow these atoms or molecules to travel unimpeded by collision, effectively reducing the mean-free path and reducing the deposition rate. Sputtering can also be performed in the presence of a small partial pressure of hydrocarbons, nitrogen, or oxygen to react with ejected atoms and form carbide, nitride, or oxide coatings in a process called reactive sputtering. It is important to note, however, that reaction between the target material and the reactive species can poison the target and interfere with deposition (Pierson, 1999).

The general disadvantages of sputtering include a relatively low deposition rate and a line-of-sight deposition characteristic which make the coating of deep holes and trenches difficult. This can be overcome to some extent by operating at higher pressure (but at some sacrifice in deposition rate) or by using three-dimensional grids. However, an advantage of sputtering is that the high energy of sputtered particles improves adhesion and produces a denser and more homogenous coating than evaporation (Pierson, 1999).

The following is a list of commonly used sputtering techniques and a description of their attributes (Pierson, 1999):

- Diode Sputtering - Simplest sputtering technique but requires an electrically conductive target, has low energy efficiency, and electron bombardment may cause significant damage of the substrate.
- Radio-Frequency (RF) Sputtering – Frequencies above 50 kHz can sputter insulators, but the process has low deposition rates.
- Triode Sputtering – An additional cathode is used to sustain the plasma, but this configuration is more complicated and may contaminate the deposit.

- Magnetron Sputtering – Magnetically enhanced cathodes (magnetrons) have considerably expanded the potential of sputtering. The magnetron sends the electrons into spiral paths to increase collision frequency and ionization. Deposition rates are high, and the process does not cause electron radiation damage.

3.1.3 Ion Plating

In ion-plating deposition, the substrate and deposited film (as it forms) are subjected to bombardment by particles (ions, atoms, molecules) which alter the formation process and properties of the coating. The process is also called ion-beam assisted deposition (IBAD) (Pierson, 1999).

Two basic versions of the ion beam plating process exist: plasma-based ion plating and vacuum-based ion plating. The coating material is vaporized in a manner similar to evaporation. Typically, the plasma is obtained by biasing the substrate to a high negative potential (5kV) at low pressure. The constant ion bombardment of the substrate sputters off some of the surface atoms which results in improved adhesion and reduced impurities. Surface coverage of discontinuities is also improved (Pierson, 1999).

Reactive ion plating is similar to reactive sputtering and evaporation with applications in optical, wear, abrasion, lubrication, and decorative coating (Pierson, 1999).

3.2 Chemical Vapor Deposition

Chemical vapor deposition (CVD), like PVD, is a vapor deposition process where the deposition species are atoms, molecules, or a combination of the two. An important recent trend is the tendency for the two processes, CVD and PVD, to merge. For instance, CVD processes now make extensive use of plasma (a physical phenomenon) and, conversely, reactive evaporation and reactive sputtering take advantage of chemical reactions in the deposition environment. Consequently, the differences between the two processes can often become blurred. Nevertheless, the CVD process may be defined as the deposition of a solid on a heated surface from a chemical reaction in the vapor phase (Pierson, 1999).

The CVD process has several important advantages that can be summarized as follows (Pierson, 1999):

- It is not restricted to line of sight, which is a general characteristic of PVD processes. The CVD process has high throwing power and can coat deep recesses, holes, and other difficult three-dimensional configurations with relative ease.
- The deposition rate is high and thick coatings (in some cases centimeters) can be readily obtained. The process is generally competitive and, in some cases, more economical than PVD processes.
- Equipment does not normally require ultrahigh vacuum and generally can be adapted to many process variations. This flexibility allows many changes in composition during deposition and the codeposition of elements or compounds is readily achieved.

The CVD process also has several disadvantages that can be summarized as follows:

- The process is most versatile at relatively high temperatures (600°C) and many substrates are not thermally stable at these temperatures. The developments of plasma-CVD and metallo-organic CVD partially offset this problem.
- Starting materials (i.e., chemical precursors) with high vapor pressures are required. These are often hazardous and at times extremely toxic. By-products of CVD reactions are also toxic and corrosive and must be neutralized, which may be a costly operation.

Although typically produced by electroplating or sputtering, CVD can be used to produce chromium coatings. Chromium is a hard metal with excellent corrosion and oxidation resistance. Chromium coatings may be produced by CVD through the pyrolysis of iodide at 700°C followed by decomposition at 1000°C or produced by hydrogen reduction of chloride at 1200° to 1350°C. Metallo-organic CVD (MOCVD) can be performed at lower temperatures (320° to 545°C) but the necessary reaction tends to incorporate carbon or hydrogen into the deposit (Pierson, 1999).

3.3 Electrodeposition

Electrodeposition is a well-established process for applying metallic coatings to improve surface properties of materials used in engineering practice. In theory, there is no limit to the thickness to which many metals and alloys can be electrodeposited, but the thickness needed to perform the required function is usually the basic criterion. Process economics are always important, and it should be noted that electrodeposition can be slow and costly. Consequently, other surfacing methods may be more appropriate when thicker coatings are desired. For thinner engineering coatings, however, electrodeposition is essential to the successful operation of innumerable components and it offers considerable scope and flexibility to the designer. The following sections provide an overview of the two main electrodeposition techniques; electroplating and electroless (aka autocatalytic) deposition (Grainger, 1998).

3.3.1 Electroplating

Electroplating involves making the component to be coated the negative electrode or cathode in a cell containing a liquid or electrolyte which must allow the passage of electric current. This electrolyte is usually a solution of water and a salt of the metal to be deposited and is maintained at a controlled temperature which can be up to about 60°C. The electrical circuit is completed by a positive electrode or anode which is generally made from the metal to be deposited and is located a short distance away from the cathode. Under the action of a direct current applied at low voltage, positively charged metal ions in the electrolyte move towards the cathode, where they undergo conversion to metal atoms and deposit on the cathode (i.e., component surface) (Grainger, 1998).

The structure and properties of the deposited metal depend on the chemical composition of the electrolyte as well as its temperature and degree of acidity or alkalinity (i.e., its pH value). These factors, and the density of the electric current per unit area of the cathode surface, determine the rate of deposition. Current flow to projections on the cathode surface is greater than to recesses, and the consequent variation in current density influences metal distribution, since the thickness deposited is proportional to the current density. Uniformity of thickness, which is a function of the throwing power of the electrolyte, can be improved considerably by attention to the design of the component and to the conditions of deposition. As electrodeposited coatings are seldom of constant thickness over the entire surface it is usual to define that portion of the surface that is essential to the serviceability of the component as the “significant surface” and to quote the minimum rather than the average thickness over this surface (Grainger, 1998).

Virtually all electrodeposition for engineering applications is undertaken in tanks or vats which may have capacities up to several thousand liters. For some specialized applications, the tank may be built around the workpiece or a large cylindrical component requiring electroplating internally may function as its own tank. The electrolyte is usually mildly agitated either by air jets or by mechanical movement of the workpiece and is maintained at the working temperature by electric immersion heaters or steam coils; alternatively, water cooling may be necessary. The anodes, suspended some centimeters from the workpiece, are sometimes inert in that they carry the current but do not dissolve in the electrolytic process, so the coating material is derived wholly from the solution. The workpiece itself is mounted on a rack or jig and suspended in the electrolyte. A transformer-rectifier set normally supplies the plating current at a voltage in the range 4-8 V. The current applied is read on an ammeter and the time to deposit

the required thickness is estimated from this current and the known efficiency of deposition (Grainger, 1998). An illustration of the vat electroplating process is shown in Figure 3-1.

Deposition efficiency is taken as the ratio of the weight of metal actually deposited against the weight that should have been deposited by the electrical energy used. Some of the current passed is usually wasted in the unavoidable evolution of hydrogen at the cathode and in resistive heating. Deposition efficiency varies with the electrolyte system in use, the plating conditions employed, and the current density (Grainger, 1998).

Non-metallic particles may also be incorporated into the metal deposit (e.g., silicon carbide in nickel) by maintaining the particles in suspension in the electrolyte. The process is controlled by measuring the density and acidity of the electrolyte and, in the longer term, by chemical analysis (Grainger, 1998).

A variation in vat plating enables small components to be plated in bulk. For example, components may be held in a perforated cylindrical barrel constructed of a polymeric material which is immersed in the plating solution and rotated continuously. The work in the barrel forms the negative electrode and in tumbling over each other, the components maintain electrical contact and simultaneously present fresh surfaces to the action of the electrolyte. Barrel plating, to which this process is often referred, is restricted to components weighing less than about 500g and are of simple shapes capable of tumbling without locking together. Coatings so applied are thin and the main applications are for decoration, but engineering applications include deposition of gold and platinum group metals for corrosion and wear resistance (Grainger, 1998).

Characteristics of Electroplating (Grainger, 1998)

1. As operation temperatures never exceed 100°C, the work should not undergo distortion or undesirable metallurgical changes.
2. Plating conditions may be adjusted to modify hardness, internal stress, and metallurgical characteristics of the deposit.
3. Coatings are dense and adherent to the substrate. Bonding, which is molecular in nature, may be as strong as 1000 N/mm^2
4. The thickness of the deposit is proportional to the current density and the length of the time of deposition.
5. As the current density over the workpiece surface is seldom uniform, coatings tend to be thicker at edges and corners and thinner in recesses and at the center of large flat areas.
6. The rate of deposition seldom exceeds 75μm/hr, but it can be accelerated by forced circulation of electrolyte.
7. There is no technical limit to the thickness of deposits. Metals such as nickel may be 13mm or more in electroforming and reclamation work, but most surfacing applications require much thinner coatings.
8. Application of coatings is not confined to the line of sight. Although the throwing power (i.e., the ability to plate around corners) may be limited, there is comparative freedom for the location of anodes, for example in the coating of bores of narrow tubing.
9. Areas not requiring deposition may be masked.

10. The size of vat limits the dimensions of the work
11. The process is suitable for automation.

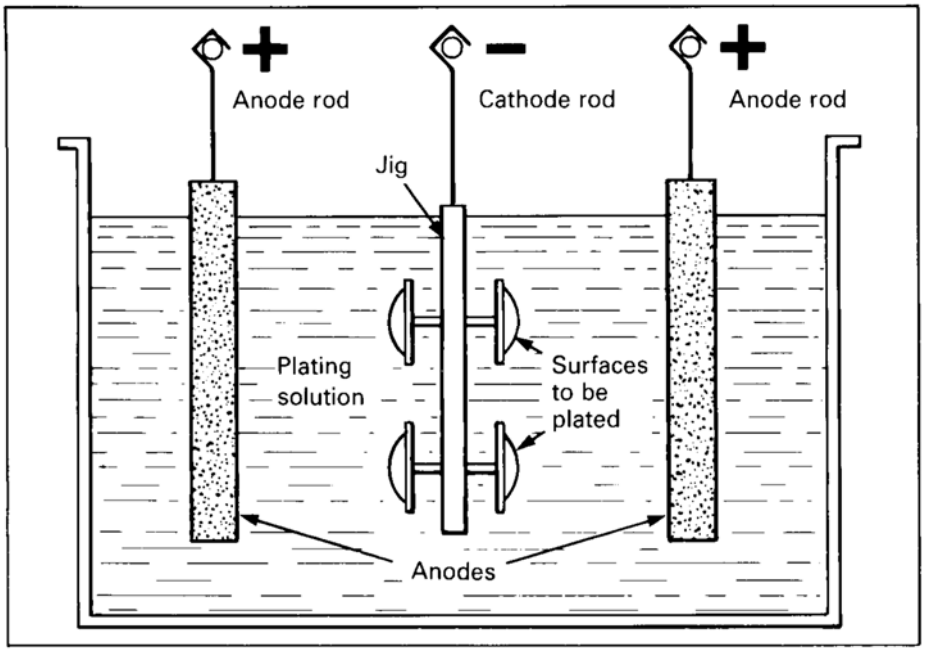

Figure 3-1. Illustration of vat electroplating process (Grainger, 1998)

3.3.2 Electroless or Autocatalytic Deposition

Electrodeposition involves the reduction of metal ions, arriving from the electrolyte, to produce metal atoms which are deposited at the cathode or workpiece surface. The current required for this reduction need not be supplied externally. By providing a reducing agent in the solution, the electrons for the deposition reaction can be furnished from within the solution. Metals such as nickel, copper, cobalt, gold, silver, and palladium can be deposited from aqueous solutions of their salts by chemical reduction and the initial layer catalyzes the subsequent deposition. Hard nickel alloys deposited from solutions containing either phosphorus or boron compounds as reducing agents are widely used in engineering. The process is generally operated in polypropylene or PTFE-coated stainless-steel tanks containing the solution maintained at about 90°C and fitted with facilities for accurate temperature control, agitation, and solution filtration. The work must be cleaned just as efficiently as in electrodeposition (Grainger, 1998).

Characteristics of electroless deposition (Grainger, 1998)

1. The equipment is simple and economical as neither anodes nor DC electrical sources are required.
2. Deposits are uniform in thickness provided that the solution can be circulated over all the surfaces to be coated. (See Figure 3-2)
3. The rate of deposition, which is dependent on temperature, is approximately 20μm/hr.
4. Thickness of up to 125-200μm can be applied.
5. Areas not requiring deposition may be masked.

6. The size of the tank limits the dimensions of the work.
7. Although chemical materials are expensive, costs may be competitive with electroplating, especially when only a few components are processed.
8. The substrate material need not be an electrical conductor.

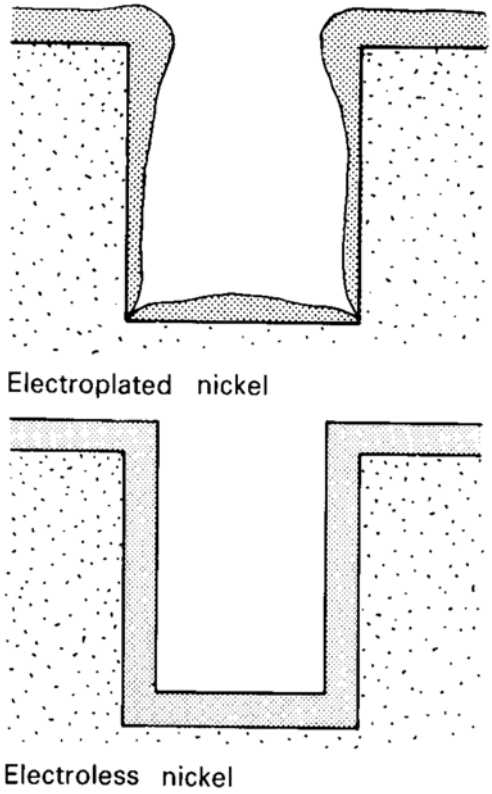

Figure 3-2. Comparison of metal distribution by electroplating and electroless deposition of nickel (Grainger, 1998)

3.3.3 Properties of Electrodeposited Chromium

Although its hardness when electrodeposited can be matched by other surface treatments, chromium possesses a unique combination of properties of value in engineering practice. The aggressive nature of the electrolytes makes the deposition of chromium alloys difficult but claims for a 1% molybdenum alloy include improved resistance to both mechanical wear and corrosion in acid environments. Characteristics of electrodeposited chromium coatings include (Grainger, 1998):

1. High hardness (i.e., 800-1000HV) conferring resistance to abrasion.
2. Low frictional coefficient and resistance to sticking, thus combating adhesive wear.
3. Resistant to corrosion, also to oxidation up to 800°C.
4. Retains room temperature strength up to about 300°C.
5. Deposits thicker than about 50μm require finishing by grinding.

6. Thickness generally limited to about 0.5mm, but thicker deposits for reclamation work are usually built up on an undercoat of nickel.
7. Brittle, not resistant to shock loading.
8. Tensile stresses are sufficiently high to induce cracking and so coating thickness should not be less than 50μm for corrosion protection.
9. The crack pattern may be developed to produce an open porous structure for lubricant retention.
10. Deposition efficiency of chromium is low and so the process is energy intensive.
11. Hydrogen discharged simultaneously may dissolve into the workpiece.

3.4 Thermal Spray

Thermal spray is a well-established, relatively low-cost, industrial process which is used widely for the deposition of metals and compounds, including refractory carbides and nitrides. The coating material, usually in the form of powder, is metered into a compressed-gas stream and fed into the heat source where it is heated to its melting point and projected onto the substrate (Pierson, 1999).

The properties of thermal-sprayed coatings vary as a function of processing parameters such as temperature and particle velocity. Generally, such coatings have greater porosity than CVD or PVD coatings and thickness control is more difficult to achieve. Nevertheless, the process is economical, undemanding, and can be applied in any location. As with reactive evaporation and sputtering, coatings of refractory compounds can be deposited reactively by spraying the pure metal in an atmosphere of either hydrocarbon or nitrogen (Pierson, 1999).

In all thermal spraying processes, the consumable coating material fed to the spray gun is raised in temperature and projected in particulate form to strike the workpiece. On arrival, the hot particles form splats which interlock and gradually build up a coating of the desired thickness. The particles must be at least partially molten in transit for splats to form. The density and cohesion of the coating depends on the material, its temperature when it strikes the workpiece, and its impact energy. These factors also impact adhesion, which is also influenced by the surface condition of the substrate. Cleaning and roughening of the workpiece is important, and alumina or silicon carbide grits are often used in place of angular iron grit as a finer particle size is preferred (Grainger, 1998).

Thermal spray processes can be divided into two categories: low energy and high energy. The low energy processes, often referred to as metallizing, include arc and flame spraying. These are extensively used for spraying metals for corrosion resistance such as zinc and aluminum, for service at or near ambient temperature, on large structures, and in circumstances where thermal and mechanical shock or abrasive wear are small. Some porosity will always be present in coatings produced through these low energy processes (Grainger, 1998).

High energy thermal spray processes include 1) Detonation gun (D-gun), which uses the energy of continuous, controlled explosions of oxyacetylene mixtures to obtain the necessary kinetic energy, 2) High-velocity oxy-fuel (HVOF), which operates at high pressure (10 MPa) and high particle velocity (ca. 315 m/s), and 3) plasma spray, which uses a DC-plasma torch or an RF inductively coupled torch. In the case of refractory metals and compound with high melting points, spraying is carried out in an inert

atmosphere to avoid detrimental chemical reactions such as oxidation (Pierson, 1999). These high energy processes were developed to provide coatings of much lower porosity and improved adhesion to the substrate. They can also handle materials of higher melting points, thus widening the range of applications to include coatings having resistance to higher temperature and to thermal and mechanical shock. With higher energy processes, the porosity is much lower and bond strengths are higher, both within the coating itself and between the coating and the substrate (Grainger, 1998).

3.4.1 Detonation Gun (D-Gun)

Detonation gun (D-gun) coating utilizes a device like a rifle barrel that has powdered coating material and an oxygen/acetylene gas mixture metered into it, which is then ignited by a spark discharge. The mixture is detonated, and the powder is propelled from the barrel at high temperatures and velocities up to 760 m/s. The operating cycle is repeated four to eight times a second to provide a continuous deposit. Because of the noise created by the process, it is carried out in a soundproof chamber and is fully automated (Grainger, 1998). A diagram of a detonation gun is shown in Figure 3-3.

Advantages of D-Gun Coatings include (Grainger, 1998):

- Very high density deposits
- High deposit adhesion
- Heavy grit blast surface preparation is not needed
- Low heat input into workpiece
- Fully mechanized and controlled process.

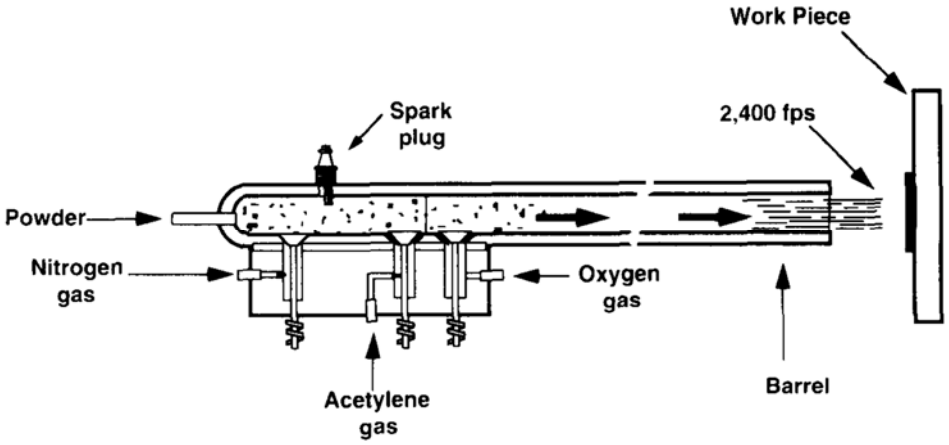

Figure 3-3. Diagram of a detonation gun (D-Gun) (Grainger, 1998)

3.4.2 High Velocity Oxy-Fuel

In HVOF systems, the combustion process is internal to the gun and the gas flow rates are much higher than in conventional flame spraying. The combination of these two factors leads to particle velocities of up to 800 m/s. A wide array of gun designs and several fuel gas options (e.g. acetylene, propylene,

propane) are available to provide desirable coatings (Grainger, 1998). A diagram of a HVOG system is shown in Figure 3-4.

Advantages of HVOF coatings include (Grainger, 1998):

- Deposits of high density and adhesion to the workpiece
- Low heat input to the component
- Tight spray pattern allows accurate placement of the deposit
- The gun to workpiece distance is relatively insensitive
- Manual or mechanized capability.

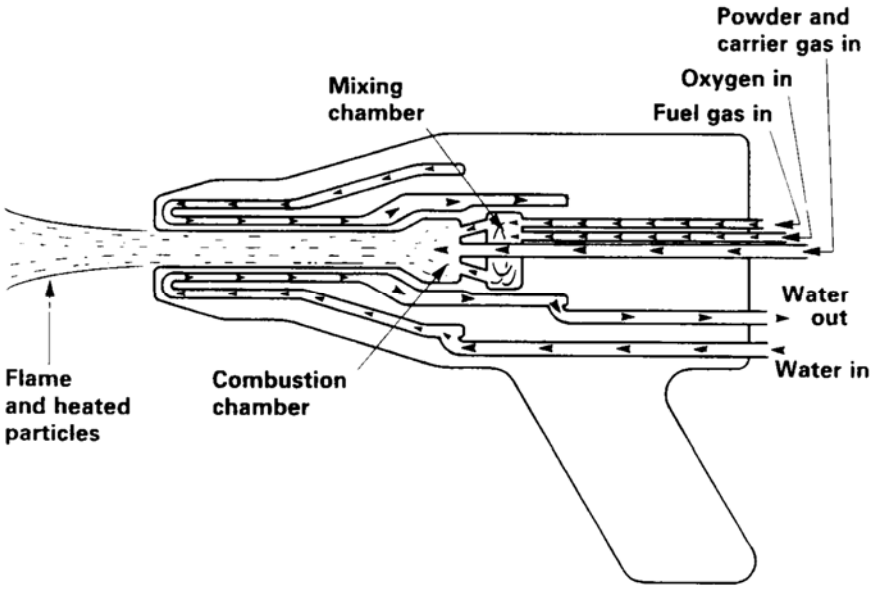

Figure 3-4. Diagram of Top Gun HVOF system (Grainger, 1998)

3.4.3 Plasma Spray

A plasma arc spray torch contains a tubular copper anode, in the rear of which is a tungsten cathode. Both electrodes are water cooled and are surrounded by an insulating body, which holds them in correct relation to each other and serves as an arc chamber. A high current arc is generated within the torch and a gas injected into the arc chamber where it is heated and, on passing through a constriction in the anode bore, is converted into a high temperature plasma. Powdered surfacing material is injected into this plasma jet and is thus heated and accelerated onto the substrate. A diagram of plasma arc spraying in air is shown in Figure 3-5.

Advantages of plasma spray include:

- The high temperature in the plasma enables almost all materials to be sprayed
- Deposits are of high density and strongly bonded to the substrate
- Very low heat input to the substrate.

Disadvantages of plasma spray include:

- Higher capital cost than low energy metallizing processes
- Deposits are of lower density and adhesion than those achieved with vacuum plasma spraying, which is essentially plasma spray in a low-pressure environment to avoid oxygen and oxidation.

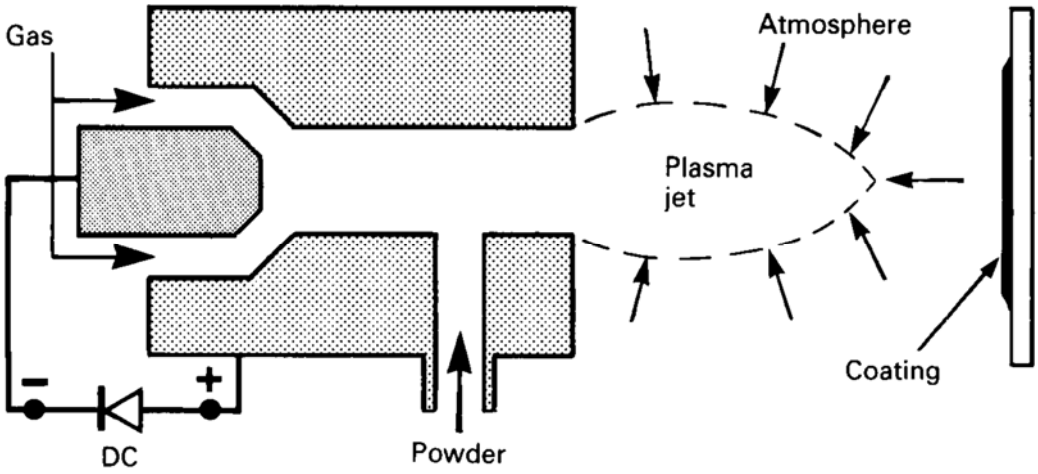

Figure 3-5. Plasma Arc Spraying in Air (Grainger, 1998)

3.5 Cold spray

Cold spraying is a fairly new technology and has attracted serious attention since unique coating properties can be obtained by the process that are not achievable by conventional thermal spraying. This uniqueness is because coating deposition takes place without exposing the spray or substrate material to high temperature and without melting the sprayed particles. Thus, oxidation and other undesired reactions can be avoided. Spray particles adhere to the substrate only because of their high kinetic energy on impact. For successful bonding, powder particles must exceed a critical velocity on impact, which is dependent on the properties of the spray material. This requires new concepts for the description of coating formation but also indicates applications beyond the market for typical thermal spray coatings. (Gärtner, Stoltenhoff, Schmidt, & Kreye, 2006)

3.5.1 Conventional High Pressure Cold Spray

This process is "a kinetic spray process utilizing supersonic jets of a compressed gas to accelerate, at or near-room temperature, powder particles to ultra-high velocities (up to 1,500 m/s). The unmolten particles traveling at speed between 500 and 1,500 m/s plastically deform and consolidate on impact with their substrate to create a coating (Fauchais, Heberlein, & Boulos, 2014).

The basis of the cold spray process is the gas-dynamic acceleration of particles to supersonic velocities and hence high kinetic energies. This is achieved using Laval (convergent-divergent) nozzles. The upstream pressure is between 2 and 2.5 MPa for typical nozzle through diameters in the range of 2-3mm. Gases used are N_2, He, or their mixtures at very high flow rates (up to $5m^3$/min). For stable conditions, typically the mass flow rate of the gas must be ten times that of the entrained powder. For a powder flow rate of 6 kg/h, this means a volumetric flow rate of 336 m^3/hr for helium and 52.3 m^3/hr for nitrogen.

Gases introduced (nitrogen or helium) are preheated up to 700-800°C to avoid their liquefaction under expansion and increase their velocity. With the highest gas flow rate this means that the heating device must be capable of heating 90m^3/min to temperature up to 700-800°C. As particles are injected upstream of the nozzle throat, the powder feeder must be at slightly higher pressure compared to the upstream chamber pressure. Especially when spraying with He, the spray is performed within an enclosure to recycle gas (Fauchais, Heberlein, & Boulos, 2014).

Particles adhere to the substrate only if their impact velocity is above a critical value. Depending on the sprayed material, this may vary between about 500 and 900 m/s. The spray pattern covers an area of roughly 20-60mm^2, and spray rates are about 3-6 kg/h. Feed stock particle sizes are typically between 1 and 50 μm and deposition efficiencies reach easily 70-90%. Only ductile metals or alloys are sprayed owing to the impact-fusion coating build-up. Blends of ductile materials (>50vol%) with brittle metals or ceramics are also used. It is important to emphasize that the substrate is not really heated by the gas exiting the gun (up to 200°C at the maximum). Current and expected application for cold spray coatings are electronic and electrical coatings, and coatings for the aircraft and automotive industries for localized corrosion protection (Fauchais, Heberlein, & Boulos, 2014).

3.5.2 Low-Pressure Cold Spray

The cost of high-pressure spray processes is rather high, especially because of the quantity of gases consumed (especially if it is helium), and the process is not adapted at all to spraying for onsite repair of parts. Portable equipment using air has been developed where the upstream pressure is below 1 MPa, typically 0.5 MPa, with a much lower gas consumption of about 0.4 m^3/min (Fauchais, Heberlein, & Boulos, 2014).

Less power is required to preheat air, which is less expensive than N_2 or He. The powder feeder can be simplified because pressurization is not necessary, and the powder can be injected downstream of the nozzle throat. With gas velocities in the 300-400 m/s range, the critical velocity of particles is not attained. To achieve coatings, small metal particles are mixed with bigger ones, which can be ceramics. Big particles mostly rebound upon impact, their role being to “press” the small metal particles onto the substrate and the previously deposited layers (shot peening effect). Powder recuperation is hardly possible for multicomponent powder mixtures. The deposition efficiency is also much lower than with high-pressure guns, but the process is attractive for short production runs (Fauchais, Heberlein, & Boulos, 2014).

3.6 Pack Cementation

Pack cementation is commonly used to apply ceramic coatings and linings to tailor the properties (e.g., mechanical, chemical, or thermal) of a substrate. This process can produce impervious, oxidation-protective coatings for refractory metals and nickel-base, cobalt-base, and vanadium-base alloys. The principal types of coatings applied by the cementation processes are silicides, carbides, and borides, usually of the base metal although frequently of codeposited or alternately deposited with other metals such as chromium, niobium, molybdenum, and titanium (American Society for Metals, 1990).

Preparation of the substrate surface for application consists of removing burrs and rounding edges and corners to prevent cracking of the ceramic coating. The next operation consists of cleaning the work

piece by vapor degreasing followed by mechanical or chemical cleaning. Mechanical cleaning is preferable, but chemical cleaning is used when the shape of the part is not suited for blasting or buffing. Parts must be rinsed and dried thoroughly after they are removed from chemical solutions, and precautions must be taken to avoid contamination of cleaned parts during subsequent handling (Fauchais, Heberlein, & Boulos, 2014).

After workpieces are prepared and cleaned, they are packed in a retort with the desired coating material. The parts should be spaced apart from each other as well as the retort walls. Parts may be layered within the retort with sufficient packing material to maintain separation. Inert filler materials may be used to provide separation and increase the efficiency with which the packing material is used. Care should be taken with handling the retort and vibrations should be minimized before and during the cementation process (Fauchais, Heberlein, & Boulos, 2014).

The packing material used in the pack cementation process usually consists of coating materials (in elemental or combined form), a suitable activator or carrier-gas-producing compound, and an inert filler material. A standard siliconizing packing material contains silicon powder, a halide salt, and an inert filler (e.g., aluminum oxide). Occasionally, urea is incorporated in the pack material to purge entrapped air before the cementation reaction begins (Fauchais, Heberlein, & Boulos, 2014).

Processing temperatures used for pack cementation coating of refractory metals depend on the substrate metal and the desired coating characteristics. In general, temperature controls the rate of deposition and time is varied to control the thickness of the coating. A low processing temperature results in a coarse, columnar structure and an uneven deposit. High processing temperatures result in deposits of uniform thickness and dense structure (Fauchais, Heberlein, & Boulos, 2014).

4.0 The Cr-Zr Phase Diagram

The substrate-coating interface must provide a sufficiently strong and stable bond throughout service to prevent delamination and benefit from the addition of the engineered coating. While some coating processes may result in a sufficiently adherent mechanical bond, many processes are conducted at elevated temperatures that result in a chemical bond at the substrate-coating interface. While chemical bonds are generally stronger and more robust than mechanical bonds, the characteristics of chemical bonds are ultimately dependent on the solid-state reactions at the interface. Cold spray and PVD are both examples of mechanical bonded coatings.

Interfacial solid-state reactions between the substrate and coating material occur in a manner similar to a diffusion couple. The resulting crystalline phase assemblage at the substrate-coating interface will influence the overall performance of the coated component and, as a result, the strength and stability of these interfacial phases is a critical aspect of an engineered coating.

Equilibrium phase diagrams of substrates and coating materials provide a convenient means of illustrating the range of crystalline phase assemblages that may be present at the interface. In addition to identifying interfacial phases, the phase diagram also provides transformation temperatures (e.g., melting, eutectic, solid-state) that may place additional limitations on the service environment of the coated component.

For chromium-coated zirconium substrates, the Zr-Cr phase diagram illustrates the equilibrium phases that may exist at the substrate-coating interface (see Figure 4.1 (Arias & Abriata, 1986)). For ceramic coatings, such a CrN or Cr_2O_3, it would be necessary to examine a ternary phase diagram to determine the equilibrium phases that could be present.

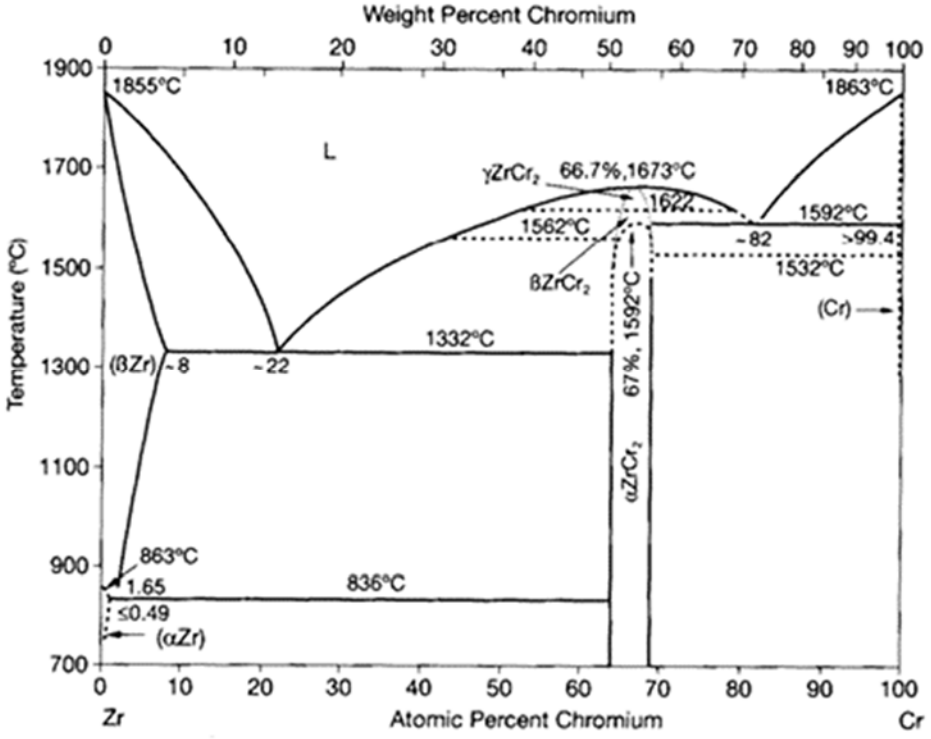

Figure 4-1. Zr-Cr Phase Diagram (Arias & Abriata, 1986)

4.1 Eutectics

A eutectic isotherm is present on each side of the $ZrCr_2$ intermetallic in the Cr-Zr phase diagram. These isotherms represent an equilibrium between the liquid phase and two solid phases. As the liquid phase cools below the eutectic isotherm, it decomposes into two solids. Conversely, the two solid phases, when in contact, will form a liquid phase when heated above the eutectic isotherm. Clearly the formation of a liquid phase below the melting points of a component's constituents has direct implications for temperature limitations on service environment and hence, understanding the temperatures of these eutectics is critical.

Of the two eutectics in the Zr-Cr phase diagram, the higher eutectic temperature occurs at 1592°C. This is also the temperature of the maximum solid solubility for Zr (< 0.6at%) in Cr. The lower eutectic temperature occurs at 1332°C and corresponds to the maximum solubility limit for Cr (8 at%) in β-Zr (Arias & Abriata, 1986). This lower eutectic temperature (1332°C) is of greater importance for establishing temperature limits for the Zr-Cr system as it represents the more limiting condition. In an engineered coating, such as a Cr-coated Zr substrate, it is possible for all phases to be present following fabrication and, depending on the service environment, these phases may form in service. Consequently, the limiting temperature to avoid liquid phase formation is set by the lower eutectic isotherm.

For ceramic coatings, such a CrN or Cr_2O_3, it would be necessary to examine a ternary phase diagram to determine the location and temperatures of various eutectics.

4.2 Brittle Phases

An intermetallic compound, $ZrCr_2$, is present in the Zr-Cr phase diagram. Intermetallic compounds generally have high melting points, low densities, and exhibit superior corrosion and oxidation resistance that make them ideal candidates for high-temperature structural materials. The $ZrCr_2$ intermetallic is a topologically close packed Laves phase of the form AB_2. Intermetallic compounds such as these are typically brittle at low temperature due to their complex crystal structure.

The intermetallic compound, $ZrCr_2$, is present in three stable phases on the Zr-Cr phase diagram. These include α, β, and γ-$ZrCr_2$, which are the low, intermediate, and high-temperature phases of the compound. The α-phase has a composition range of 64-69 at% Cr at 900°C and transforms to the β-phase at about 1592°C. The high temperature γ-phases is only stable between 1622°C (β to γ transformation) and its congruent melting temperature (1673°C). It should be noted that severe experimental difficulties are found in the $ZrCr_2$ compositional range due to the long times and high temperature required to attain stable equilibrium. Consequently, the details of the β + γ phase region of the Cr-Zr phase diagram is incomplete and rather speculative (Arias & Abriata, 1986). This would only be a concern above 1592°C

The intermetallic compound, $ZrCr_2$, can form due to diffusion of atoms in the Zr substrate and Cr atoms in the coating. The formation of this intermetallic has been observed with a thickness of 4 μm after 66 hours at 775°C (Sweeney & Batt, 1964). The formation of this intermetallic has also been observed with a thickness between 1 and 4.5 μm after 49 to 225 hours at 750°C to 850°C (Wenxin & Shihao, 2001). Based on these thickness measurements an equation for the diffusivity of Cr in Zr was derived as:

$D = 6.27 \times 10^{-12} \exp(-1.26 \times 10^5 / RT)$ (m^2/s)

where T is in K and R is in J/mol-K (Wenxin & Shihao, 2001).

Using this diffusivity, the following predictions were made for normal conditions and accident conditions:

- Normal Conditions (300°C-350°C for 2000 days) 0.1 to 0.3 μm thick intermetallic layer
- Loss-of-coolant Conditions (800 to 1200°C for 1 hour) 0.2 to 1.4 μm thick intermetallic layer
- Long term Loss-of Coolant (800 to 1200°C for 1 day) 1 to 7 μm thick intermetallic layer.

This diffusion is expected to occur for any coating technique where the coating and substrate are in intimate contact. Additionally, diffusion can often be accelerated in an irradiation field, so intermetallic layers could be thicker in practice. Mechanical testing would have to be performed to determine what the impact on ductility would be of various thicknesses of this intermetallic.

A study on $ZrCr_2$ performed by Ohta (Ohta, Nakagawa, Kaneno, & Kim, 2003) compared the microstructure and mechanical properties of $ZrCr_2$ samples generated by ingot metallurgy (as-cast) and powdered metallurgy. Although the as-cast $ZrCr_2$ prepared by arc melting may contain residual high temperature C14 (γ, hexagonal) or metastable C36 (β, di-hexagonal) phases, these phases were consumed by the C15 (α, cubic) phase upon subsequent annealing. Compressive strength measurements performed in vacuum at ~1030°C revealed a 0.2% yield stress of ~600 MPa that decreased to ~200 MPa at 1127°C for $ZrCr_2$ samples formed by powdered metallurgy while the strength of as-cast samples was ~300 MPa at 1400K (Ohta, Nakagawa, Kaneno, & Kim, 2003). Hardness and fracture toughness measurements were performed via Vickers micro-indentation and ranged between 850 and 900 HVN and 1 and 3 MPa√m, respectively, for the powdered metallurgy and as-cast $ZrCr_2$ samples. Thermogravimetric measurements performed in air at 950°C for 48 hrs revealed parabolic oxidation of $ZrCr_2$ prepared by powdered metallurgy. It was noted that increased Cr content increased the oxidation rate (Ohta, Nakagawa, Kaneno, & Kim, 2003), which is counterintuitive as Cr is typically added to promote the formation of a protective oxide layer.

High temperature oxidation of arc-melted $ZrCr_2$ was evaluated by Oryshich over the temperature range of 600 to 1200°C. The motivation for this study was to determine the suitability of various intermetallics for creating composite alloys and coatings for high temperature environments. In Oryshich's opinion, the oxidation behavior of an intermetallic is typically similar to the base material (e.g., Zr). However, the rate of $ZrCr_2$ oxidation was observed to be linear and catastrophic (would quickly lead to cladding failure) above 600°C. Oryshich reasoned that this was due the higher affinity of Zr for oxygen relative to Cr and the less protective properties of the Zr oxide. This resulted in the formation of a brittle oxide scale composed of Zr and Cr oxides as opposed to a protective Cr oxide layer. Thermal expansion mismatch between the oxides resulted microcracking, which resulted in a porous, friable scale. (Oryshich, Poryadchenko, & Brodnikovskii, 2004).

Oxidation studies of vacuum arc melted Zr-Cr alloys were also conducted over a temperature range of 500 to 700°C by Brodnikovskii et al. for alloys containing between 0.5 and 8% at% Cr. The addition of Cr in Ti and Zr alloys is known to enhance strength and creep properties, but the aim of this study was to determine the effects of Cr addition on oxidation resistance. The oxidation resistance of the alloys was significantly decreased with increasing Cr concentration and temperature. It was recommended that

zirconium alloys with 8 at% Cr be restricted to use at temperatures below 500°C and that the chromium content be restricted to less than 4 at% if intended for use at 600°C. The oxidation rates appeared to be parabolic under these conditions but became intermediate between parabolic and linear with increased temperature or Cr concentration and temperature (Brodnikovskii, et al., 2010).

4.3 Summary

The binary phase diagram was presented for the Zr-Cr system. This phase diagram is useful for predicting the presence of various intermetallic phases that can exist as Zr and Cr diffuse together, as well as the location where low temperature eutectic formation can cause localized melting below the melting temperature of either metal separately. For ceramic coatings, a ternary phase diagram would have to be obtained or developed to predict these parameters for that system.

For the binary Zr-Cr systems a low temperature eutectic of 1332°C has been identified. Although current LOCA limits constrain the cladding to 1204°C, this limit should be considered if operation of accident tolerant fuels above this limit was considered. For ceramic coatings, a ternary phase diagram would have to be obtained or developed to determine if this low temperature eutectic would still exist or if others would exist.

If Cr and Zr interdiffusion were to occur, it is likely that the $ZrCr_2$ phase which may be brittle and lead to overall cladding embrittlement. Additionally, this phase has been observed to have poor corrosion resistance at 500°C and 600°C. Additional work is necessary to quantify the amount of Zr-Cr interdiffusion is required for either of these effects to cause overall cladding embrittlement or loss of corrosion protection.

5.0 Changes to Safety Analysis Codes, Methods, and Limits for Cr-coated Zr Cladding

For a fuel vendor to be able to perform cycle specific safety analyses on a new fuel assembly design that deviates from limits applied to their currently approved methodologies, that vendor would typically prepare and submit new licensing topical reports (LTRs) to the NRC to describe the codes and methods that would be used to perform these analyses. Alternatively, the fuel vendor could prepare and submit supplements to existing LTRs that state changes to the codes and methods that would be used to perform safety analyses for the new fuel assembly design.

This second approach is the approach that has typically been used when introducing new proprietary cladding alloys such as ZIRLO, Optimized ZIRLO, M5®, and ZIRON, which are evolutionary changes from Zircaloy-4 and Zircaloy-2. The content of these LTR supplements describes the material property correlations that will be used for the new cladding alloy along with data to justify the use of each correlation. Even in the case where an existing correlation will be used for the new cladding alloy, some justification, preferably citing data, that the use of the correlation is appropriate, should be provided. It is the responsibility of the applicant to propose specified acceptable fuel design limits (SAFDLs) for their analyses and justify those limits. Because of this, these LTR supplements also state these limits and provide relevant data that demonstrate that these limits will adequately protect the fuel assembly. Finally, if any changes are made to the analytical methodology to perform the safety analyses for the new cladding alloy, these changes will also be described in the LTR supplement or similar licensing document.

This approach of licensing the use of a new cladding alloy can be used as a model for the introduction of coated cladding. The same review and approval will be required of any licensing requests in the following three areas:

- Material property correlations to be used in codes for new cladding
- SAFDL limits for new cladding
- Any changes to existing methodology for new cladding.

This section is intended as a guide for the NRC staff as they perform a review of an LTR, LTR supplement, or license amendment request related to the implementation of Cr-coated cladding. Section 5.1 provides a list of cladding material property correlations that are typically needed to adequately model fuel system response based on development and qualification of NRC's independent fuel performance code, FRAPCON (Geelhood K. , Luscher, Raynaud, & I.E., 2015) and based on all previously approved thermal mechanical codes. This section also identifies data that are typically used to develop and justify these correlations. Section 5.2 discusses SAFDL limits in areas that are identified in Standard Review Plan Section 4.2 (US Nuclear Regulatory Commission, 2007). This section also identifies data that are typically used to develop and justify these limits. This section will also identify potential new damage mechanisms that should be considered specifically for Cr-coated cladding along with data that could be used to justify proposed limits. Section 5.3 discusses potential changes to existing codes and methodologies that may be enacted to perform safety analyses for Cr-coated cladding.

There are two basic approaches that an applicant could use during the update of their codes and methods for Cr-coated cladding. Each of these is discussed briefly below but should be considered in the following sections.

The first approach is to consider the coating separate from the cladding. In this approach the base Zr-alloy cladding would be considered already approved and updated codes and methods would be used to model the impact of the coating on the performance. This approach may be more difficult because additional modeling would be needed to model the impact of the coating on performance of the cladding. Models for the cladding coating interface would be necessary as well as models to combine the strength and creep properties of each material into an effective strength and creep rate. Finally, it would be reasonable to include data from the coated cladding to demonstrate that the modeling effectively represents the behavior of the coated cladding.

The second approach would be to treat the coated cladding as a composite material and develop correlations for thermal and mechanical properties based on tests performed on representative coated cladding specimens. This approach may be more straightforward as additional modeling may not be necessary and material properties can be developed from fully representative samples. This approach could also attempt to make an argument to ignore the coating in the analyses and rely on existing cladding properties.

5.1 Cladding Material Property Correlations

The following cladding material properties are typically needed to perform fuel thermal-mechanical analysis of nuclear fuel with Zr-alloy cladding under normal conditions and AOOs:

- thermal conductivity
- thermal expansion
- emissivity
- enthalpy and specific heat
- elastic modulus
- yield stress
- thermal and irradiation creep rate
- axial irradiation growth
- oxidation rate
- hydrogen pickup.

The following additional material properties are typically needed to perform fuel-mechanical analysis of nuclear fuel under accident conditions based on the development and qualification of the NRC transient fuel performance code, FRAPTRAN (Geelhood K. , Luscher, Cuta, & Porter, 2016):

- High temperature ballooning behavior
- High temperature (800-1200°C) steam oxidation rate.

If the first approach discussed above to independently model the coating and the cladding is taken, then each of the above properties and the impact of irradiation on these should be determined as well as the interface behavior. If the second approach discussed above to model the cladding and the coating as a composite material is taken, then the impact of the coating on the base metal should be determined. The following discussion provides information on the potential impact of a metallic or ceramic coating on the base metal.

Each of these properties are discussed in the following sections as they relate to Cr-coated Zr cladding. The type of data that are typically used to justify each property will be stated. Currently it is not possible to definitively state what data are available to justify these properties, because small differences in vendor specific processes can have a significant impact on the properties. Therefore, the applicant should provide data or other justification from their specific cladding product to justify material property models. There is a growing body of generic data from various Cr-coated Zr samples as discussed in Section 6.0. These data are important because they provide the NRC staff a baseline of what to expect when reviewing an application and claims of large deviations from the generic database may indicate an area for a more detailed review. In the following discussion it should be noted that the coatings under consideration are 5 to 30 microns thick on cladding that is 500 to 700 microns thick. Table 5.1. provides a summary of the tests that could be performed to quantify the material properties discussed below.

5.1.1 Thermal Conductivity

Zr-alloy Cladding

Cladding thermal conductivity is not expected to change significantly with irradiation based on the currently available data. Typically heat transfer in a metal is due to electronic heat transfer which is not significantly impacted by lattice damage done by fast neutron irradiation. No change in thermal conductivity with irradiation is used in FRAPCON (Luscher, Geelhood, & Porter, 2015). Thermal conductivity data as a function of temperature from unirradiated samples have typically been used to develop cladding thermal conductivity correlations.

Cr-coated Zr

Either an effective thermal conductivity for the coated cladding could be developed or a method for combining the thermal conductivity from the base metal and the coating could be described. The thermal conductivity of Cr metal is not expected to be strongly impacted by irradiation. The thermal conductivity of a Cr-based ceramic may be impacted by irradiation. It is possible that the overall cladding thermal conductivity may not be strongly impacted by this as the coating is expected to be relatively thin. This would be similar to the treatment of the ZrO_2 that evolves on the surface of the Zr-alloy cladding.

5.1.2 Thermal Expansion

Zr-alloy Cladding

Cladding thermal expansion is not expected to change significantly with irradiation based on the currently available data. Thermal expansion is caused by crystal lattice expansion and does not change much with the introduction of dislocations from fast neutron irradiation. No change in thermal expansion with irradiation is used in FRAPCON (Luscher, Geelhood, & Porter, 2015). Thermal expansion data as a

function of temperature from unirradiated samples have typically been used to develop cladding thermal expansion correlations.

Cr-coated Zr

Typically, the thermal expansion of a coated part will be the same as that of an uncoated part if the coating is relatively thin. However, thermal expansion data from representative cladding tubes would be useful to justify the correlation and to demonstrate that there has not been a change in behavior with the coating due to thermal expansion mismatch between the substrate and the coating. Thermal expansion mismatch between a coating and substrate typically results in plastic strain in the thin coating which is weaker than the substrate because of its thickness. Many ceramics have a limited strain capability. A ceramic coating with a significant thermal expansion mismatch strain may exhibit cracking upon heating and cooling due to the inability of that coating to tolerate plastic strain.

5.1.3 Emissivity

Zr-alloy Cladding

Cladding emissivity is important to calculate the portion of the gap heat transfer due to radiative heat transfer. The emissivity is impacted by the surface conditions including any oxide on the surface of the cladding.

Cr-coated Zr

The gap heat transfer occurs on the inner surface of the tube and will not be impacted by the coating on the outer surface. Some system codes and accident analysis codes account for cladding surface emissivity and radiation heat transfer from fuel rods to other reactor core components. The outer surface emissivity may be important in severe accident analysis or even in design basis accident analysis (especially if licensees propose higher peak cladding temperature limits for their plants). Because the current coatings are on the outer surface it would be acceptable to retain the emissivity used for an uncoated Zr alloy tube for thermal-mechanical analysis, but it may be necessary to revise the outer surface emissivity for accident analyses. This would apply equally to metallic and ceramic coatings.

5.1.4 Enthalpy and Specific heat

Zr-alloy Cladding

Cladding enthalpy and specific heat are not expected to change significantly with irradiation based on the currently available data. Specific heat of a material is dependent on the composition and the crystal structure and does not change much with the introduction of dislocations from fast neutron irradiation. No change in enthalpy or specific heat with irradiation is used in FRAPCON (Luscher, Geelhood, & Porter, 2015). Enthalpy and/or specific heat data as a function of temperature from unirradiated samples would be useful to develop cladding enthalpy and specific heat correlations.

Cr-coated Zr

Either an effective enthalpy and specific heat for the coated cladding could be developed or a method for combining the enthalpy and specific heat from the base metal and the coating could be described. Cladding enthalpy and specific heat are only needed for transient fuel performance analysis and for calculation of stored energy. This would apply equally to metallic and ceramic coatings.

5.1.5 Elastic Modulus

Zr-alloy Cladding

Cladding elastic modulus has been observed to be a weak function of fast neutron fluence (proportional to fuel burnup) (Geelhood, Beyer, & Luscher, PNNL Stress/Strain Correlation for Zircaloy. PNNL-17700, 2008). Not all applicants include a fluence dependence, but if one is included, then temperature dependent data from irradiated and unirradiated coated tubes would be useful to justify the correlation used.

Cr-coated Zr

Recent data on unirradiated Cr-coated Zr indicate the elastic modulus of a coated part will be the same as that of an uncoated part (Brachet, et al., 2017) (Kim, et al., 2015) (Shahin, Petrik, Seshadri, Phillips, & Shirvan, 2018). Typically, ceramic materials are stiffer (greater elastic modulus) than metallic materials. However, for thin coatings the enhanced stiffness of the coating is not expected to strongly impact the overall stiffness of the substrate.

5.1.6 Yield Stress

Zr-alloy Cladding

Cladding yield stress has been observed to be a strong function of fast neutron fluence (proportional to fuel burnup) early in life and saturates to a value at moderate fluence levels. Temperature dependent data from irradiated and unirradiated coated tubes should be provided to justify the correlation used.

Cr-coated Zr

Recent data on unirradiated Cr-coated Zr indicate the yield stress of a coated part will be the same as that of an uncoated part (Brachet, et al., 2017) (Kim, et al., 2015) (Shahin, Petrik, Seshadri, Phillips, & Shirvan, 2018). In tension, ceramic materials display a wide variation in strength. However, for thin coatings the variable strength of the coating is not expected to strongly impact the overall strength of the substrate.

5.1.7 Thermal and Irradiation Creep Rate

Zr-alloy Cladding

The creep behavior of zirconium alloy tubes has often been characterized by a thermal rate which can be developed based on ex-reactor creep tests, which are a function of stress and temperature, and an

irradiation rate which can be developed based on the additional creep observed at the same stress and temperature during an in-reactor creep test. This creep rate can change significantly with small changes to alloy composition or microstructure. The increase or decrease in the thermal creep rate does not directly correlate to an increase or decrease in the irradiation creep rate. One example of this is the creep rates for recrystallized cladding and stress-relief annealed cladding in FRAPCON. Although both the thermal and irradiation creep rates are greater for the stress-relief annealed cladding than the recrystallized cladding, the two increases are not the same fraction so one increase could not be determined from the other (Geelhood K. , Luscher, Raynaud, & I.E., 2015) (Limback & Andersson, 1996). Both in-reactor and ex-reactor creep tests are recommended to justify the cladding creep correlation used as these processes are potentially controlled by different mechanisms.

Cr-coated Zr

Recent data on unirradiated Cr-coated Zr indicate the thermal creep behavior of a coated part will be the same as that of an uncoated part (Brachet, et al., 2017). A thin metallic or ceramic coating on the cladding is unlikely to impact the thermal or irradiation creep behavior of the substrate. However, as mentioned above, small changes in composition and microstructure can have a significant impact on creep behavior, such that the *application* of the metallic or ceramic coating may impact the creep behavior. For this reason, both in-reactor and ex-reactor creep tests are recommended to justify the cladding creep correlation used for Cr-coated Zr cladding.

5.1.8 Axial Irradiation Growth

Zr-alloy Cladding

Zirconium alloy tubes have been observed to grow axially with increased fast neutron fluence (Luscher, Geelhood, & Porter, 2015). This growth rate can change significantly with small changes to alloy composition or microstructure (for example, Zircaloy-2, Zircaloy-4, M5®, ZIRLO). In-reactor data would be useful to justify the axial growth correlation used.

Cr-coated Zr

There is no current experience with the axial irradiation growth of coated parts relative to uncoated parts. Like thermal expansion mismatch strain, a difference in growth rates between the coating and substrate could lead to plastic deformation in the coating. This could be especially exacerbated for ceramic coatings as ceramics typically have low plastic strain capability. Large differences in growth rate between the cladding and coating could lead to cracking or adhesion issues.

5.1.9 Oxidation Rate

Zr-alloy Cladding

The oxidation rate is important to model in uncoated cladding tubes as the zirconium oxide layer is less conductive than Zr metal. In the zirconium alloy systems, ex-reactor autoclave corrosion data is significantly different from in-reactor corrosion data and should not be used to develop corrosion correlations for coated parts. Additionally, the corrosion behavior of non-fueled cladding segments may also not be representative of fueled cladding corrosion as the surface heat flux in the fueled cladding

seems to strongly impact oxidation rate (Cox, 2005) (Sabol, Comstock, Weiner, Larouere, & Stanutz, 1993) (Garde, Pati, Krammen, Smith, & Endter, 1993).

Cr-coated Zr

The Cr coatings under consideration will most likely result in very low oxidation rates under normal conditions and AOOs. Both the metallic and ceramic Cr coatings produce a protective chromium oxide layer that exhibits excellent corrosion resistance. Some in-reactor data from fueled rods under prototypical coolant conditions are recommended to demonstrate the oxidation rate or lack of one.

5.1.10 Hydrogen Pickup

Zr-alloy Cladding

It is important to quantify the hydrogen pickup in uncoated cladding tubes as hydrides in zirconium can lead to brittle behavior of the cladding (Zhao, et al., 2017).

Cr-coated Zr

In the case of Cr-coated Zr, if it is demonstrated that the metallic or ceramic Cr-coating leads to negligible oxidation and is a barrier to hydrogen pickup, then this might not be necessary for Cr-coated Zr cladding tubes.

5.1.11 High Temperature Ballooning Behavior

Zr-alloy Cladding

The burst stress as a function of temperature is important to know for LOCA analysis as this will determine when to start two-sided oxidation. The ballooning strain is important to determine flow blockage and establish if a coolable geometry has been maintained. Ex-reactor burst tests at temperatures of interest for LOCA on representative cladding segments have been used in the past to establish the high temperature ballooning behavior of Zr-alloy tubes (Powers & Meyer, 1980).

Cr-coated Zr

Burst stress and ballooning strain are especially important for Cr-coated cladding as the Cr coating is expected to provide a barrier to high temperature oxidation, but it has not been proposed to coat the inner surface of the tube, so once ballooning and burst has occurred there will be at least some bare Zr available for reaction with high temperature steam.

Ex-reactor burst tests at temperatures of interest for LOCA on representative cladding segments would be useful on metallic or ceramic Cr-coated Zr alloy tubes to quantify the ballooning and burst behavior.

5.1.12 High Temperature Steam Oxidation Rate

Zr-alloy Cladding

The steam oxidation rate is important for LOCA analysis because this determines if the cladding has been overly thinned by corrosion. This also determines the extra heat generation from the corrosion reaction.

Cr-coated Zr

Ex-reactor oxidation tests at temperatures of interest for LOCA on representative cladding segments have been used to establish the high temperature steam oxidation rate of Zr-alloy tubes. Such data would be useful on either metallic or ceramic Cr-coated Zr alloy tubes to quantify the oxidation rate.

Table 5.1. Tests that could be used to quantify property correlations for Cr-coated Zr alloy tubes

Property	Recommended Tests
Thermal conductivity	Tests on unirradiated cladding samples over representative temperature range
Thermal expansion	Tests on unirradiated cladding samples over representative temperature range
Emissivity	None
Enthalpy and specific heat (only needed for transient analysis and calculation of stored energy)	Tests on unirradiated cladding samples over representative temperature range
Elastic Modulus	Tensile tests on irradiated cladding tubes over a representative range of burnup and temperatures
Yield Stress	Tensile tests on irradiated cladding tubes over a representative range of burnup and temperatures
Thermal and irradiation creep	In-reactor creep tests on pressurized cladding tubes over a representative range of burnup and temperatures
Axial irradiation growth	Poolside length measurements from LTAs over a representative range of burnup and temperatures
Oxidation rate	Poolside eddy current measurements from LTAs over a representative range of burnup and temperatures
Hydrogen pickup	Destructive examination of cladding segments from LTAs

High temperature ballooning behavior	Ex-reactor burst tests at relevant temperature. Unirradiated samples are acceptable
High temperature steam oxidation rate	Ex-reactor corrosion tests at relevant temperature. Unirradiated samples are acceptable

5.2 SAFDL Limits for New Cladding

The previous section discussed the cladding material properties that are typically needed to perform the required thermal-mechanical safety analyses. The second step is determining the specified acceptable fuel design limits (SAFDLs). The NRC Standard Review Plan section 4.2 identifies several general phenomena that should be considered for standard fuel and cladding to avoid fuel system damage and fuel rod failure and to ensure fuel coolability. The standard review plan also provides some general guidance in selecting specific limits in each area. However, it is the responsibility of the applicant to propose and justify the specific limit that should be used in each area. It is also the responsibility of the applicant to identify and propose limits for possible damage mechanisms that have not been identified by the standard review plan.

To provide assistance to NRC staff during the review of an LTR or LTR supplement regarding Cr-coated Zr cladding, this section discusses the expected impact of the Cr-coating on typical limits for Zr-alloy cladding and the data that would likely need to be collected to justify a revised limit. This section also identifies new damage mechanisms that should be considered for Cr-coated Zr cladding and identifies data collection that could be used to justify a new limit.

The SAFDLs mentioned in the Standard Review Plan are broadly separated into three general categories:

- SAFDLs related to assembly performance that are typically addressed by simple calculation, manufacturing controls, and historical data
- SAFDLs related to fuel rod performance that are typically addressed for normal operation and AOOs using a thermal mechanical code
- SAFDLs related to fuel rod performance that are typically addressed for accident conditions using a system analysis code with initial conditions provided by a thermal mechanical code.

Table 5.2 lists each of the SAFDLs mentioned in the Standard review plan in each of these three general categories. Also shown in this table is the purpose of each established limit.

Table 5.2 SADFLs from the standard review plan and the purpose of each limit

SAFDL Category	SAFDL	Purpose of Limit
Assembly Performance	rod bow	Could impact DNBR or MCPR
	irradiation growth	Excessive assembly growth could lead to assembly deformation
	hydraulic lift loads	The weight of the assembly and force of holddown springs should prevent assembly liftoff
	fuel assembly lateral deflection	Lateral deflections should not be so great as to prevent control rods/blades from being inserted
	Fretting wear	Excessive fretting wear can lead to failed cladding
Fuel rod performance (normal operation and AOO	cladding stress	Prevent failure of cladding from overstress conditions
	cladding strain	Prevent failure of cladding from excessive strain conditions
	cladding fatigue	Prevent failure of cladding from cyclic fatigue
	cladding oxidation, hydriding and CRUD	Prevent oxide spallation which can result in formation of brittle hydride lens Retain cladding ductility as stated in cladding strain limit
	rod internal pressure	Prevent cladding liftoff due to overpressure during normal operation Prevent reorientation of the hydrides in the radial direction in the cladding which can embrittle the cladding (protect strain limit) Prevent significant deformation resulting in departure of nucleate boiling (DNB)
	internal hydriding	Retain cladding ductility as stated in cladding strain limit
	cladding collapse	Prevent failure of cladding due to collapse in the plenum and axial pellet gaps which results in large local strains
	overheating of fuel pellets	Prevent fuel melting to assure that axial or radial relocation of molten fuel would neither allow molten fuel to contact the cladding nor produce local hot spots.
	pellet-to-cladding interaction	Prevent cladding failure from chemically assisted cracking

SAFDL Category	SAFDL	Purpose of Limit
Fuel rod performance (accident conditions)	overheating of the cladding	Failure of cladding and dose consequence if critical heat flux is exceeded
	excessive fuel enthalpy	Failure of cladding and dose consequence during RIA if injected energy limit is exceeded
	bursting	Time of burst during LOCA needed for oxidation of inner cladding and associated heat is correctly modeled
	mechanical fracturing	Failure of cladding and dose consequence from external event
	cladding embrittlement	Coolable geometry must be retained following LOCA
	violent expulsion of fuel	Coolable geometry must be retained following RIA. Pressure pulse must not damage reactor vessel
	generalized cladding melting	Coolable geometry must be retained following LOCA
	fuel rod ballooning	Degree of ballooning needed to calculate blockage of the coolant channel
	structural deformation	Coolable geometry must be retained following LOCA or seismic event

The existing SAFDLs and any additional concerns are described in the following sections, which are devoted to each one of the three general categories above. Table 5.3 provides a summary of the tests that could be performed to justify the SAFDLs discussed below beyond what was necessary to quantify the material property correlations.

5.2.1 SAFDLs Related to Assembly Performance

SAFDLs related to assembly performance are typically performed by simple hand calculations or by siting manufacturing controls or historic data. These limits may need revision relative to those typically used for Zr-alloy tubes.

5.2.1.1 Rod Bow

Usually there is a penalty on departure from nucleate boiling ratio (DNBR) or margin to critical power ratio (MCPR) to account for bowing. The limits of what degree of bowing is acceptable will not change with the introduction of Cr-coated Zr as this is controlled by the physical dimensions of the fuel assembly. However, bowing methods rely on correlations that are very empirical. Some testing or

assessment would be useful to assess the applicability of the rod bow correlation used for Cr-coated cladding.

5.2.1.2 Irradiation Growth

The assembly design allows for a given amount of growth and will define the limit. The axial growth from Section 5.1.8 will be used to assess maximum growth. There are currently no additional concerns that need to be addressed regarding irradiation growth for Cr-coated Zr cladding.

5.2.1.3 Hydraulic Lift Loads

The limits for hydraulic lift loads are such that the upward hydraulic forces do not exceed the weight of the assembly and the downward force of the holddown springs. None of these parameters are expected to change with the introduction of Cr-coated Zr cladding. Existing limits and methods are expected to be adequate.

5.2.1.4 Fuel Assembly Lateral Deflections

The limits for fuel assembly lateral deflections are such that the control rod (PWR) or control blades (BWR) can still be inserted as needed. Current assembly and channel bow methods are used to assess performance relative to these limits. Assembly and channel bow are not impacted by fuel rod performance, but rather by channel design (BWR) and guide tube design (PWR) and therefore these limits and methods are not expected to change with the introduction of Cr-coated Zr cladding tubes.

5.2.1.5 Fretting Wear

Current design limits state that fuel rod failures will not occur due to fretting. Fretting has historically been controlled though debris filters that reduce the possibility for debris fretting and through spacer design to reduce fretting between fuel rods and grid features. Ex-reactor fretting tests on unirradiated Cr-coated Zr cladding tubes would be useful to ensure that fretting behavior will not be an issue with the coating. A concern for Cr-coated Zr is that grid features are not damaged by the hard coating on the fuel rod. Ex-reactor fretting tests could be used to demonstrate that grids are not damaged by the hard coating on the fuel rod.

5.2.2 SAFDLs Related to Rod Performance Assessed for Normal Operation and AOOs

Current codes that are informed by the properties in Section 5.1 can perform the following analyses. However, the limits may need revision relative to those typically used for Zr-alloy tubes.

5.2.2.1 Cladding Stress

Cladding stress limits are typically set using a method described in Section III of the ASME code (American Scociety of Mechanical Engineers, 2017). Typically, these limits are based on unirradiated yield stress to represent the lowest yield stress. For Cr-coated Zr, the use of the unirradiated yield stress determined in Section 5.1.6 should be acceptable to determine a stress limit.

5.2.2.2 Cladding Strain

There are two cladding strain limits that are typically employed. The first steady-state limit is the maximum positive and negative deviation from the unirradiated conditions that the cladding may deform throughout life. The second transient strain limit is the maximum strain increment caused by a transient. These cladding strain limits are typically justified based on mechanical tests (axial tension tests and tube burst tests) performed on irradiated cladding tubes. Ductility tends to decrease with irradiation (Geelhood, Beyer, & Luscher, 2008), so these tests are most relevant when performed at the maximum expected fast neutron fluence. The uniform elongation or strain away from the rupture has been typically used as the strain capability for Zr-based alloys (Geelhood, Beyer, & Cunningham, 2004). This would be a good metric for Cr-coated Zr cladding to protect against cladding mechanical failure. For Cr-coated cladding, there is the additional concern that large strains in the cladding may lead to cracking of the coating (See Section 6.3.1). Cracking of the coating can lead to a loss of corrosion protection for the substrate along with delamination. The authors propose adding crack detection criteria so that there is no visual cracking or microcracking of the coating

5.2.2.3 Cladding Fatigue

The cladding fatigue limit is typically based on the sum of the damage fractions from all the expected strain events being less than 1.0. The damage fractions are typically found relative to the O'Donnell and Langer irradiated fatigue design curve (O'Donnell & Langer, 1964). It is currently unknown if the O'Donnell and Langer irradiated fatigue design curve would be applicable to Cr-coated Zr. It has been noted (Kvedaras, Vilys, Ciuplys, & Ciuplys, 2006) that in steels, Cr coating can improve or significantly worsen the fatigue lifetime due to different microstructures produced in the coating. This was also observed in the case of Cr-coated Zr where the fatigue life went down with the application of a coating (Sevecek, et al., 2018). Because of this, fatigue data from irradiated cladding that was produced using a representative process for the applicant in question is recommended to either confirm the O'Donnell and Langer irradiated fatigue design curve or to develop a new fatigue design curve. New fatigue design curves should include a safety factor of 2 on stress amplitude or a safety factor of 20 on the number of cycles as mentioned in the Standard Review Plan Section 4.2.

5.2.2.4 Cladding Oxidation, Hydriding, and CRUD

For Zr-alloy cladding, the cladding oxidation limit is designed to preclude oxide spallation that has typically been observed above 100 μm. Oxide spallation can lead to a local cool spot which acts as a sink for hydrides, creating a local, extremely brittle hydride lens. The hydrogen limit is designed to ensure that the strain limit previously identified will be applicable since high levels of hydrogen (>600ppm) can cause embrittlement of the cladding. Hydrogen is not the only embrittlement mechanism and there may be other embrittlement mechanisms that are discussed elsewhere. There is no explicit limit on CRUD, other than it be explicitly considered if it is present and it is typically modeled as an insulating layer around the fuel rod in plants that have CRUD issues.

None of these limits are particularly relevant to Cr-coated cladding since the outer oxide will be Cr_2O_3 rather than ZrO_2 and the Cr and/or Cr_2O_3 are expected to be a barrier against hydrogen uptake. Limits should be proposed that preclude environmental damage to the protective Cr_2O_3 layer and embrittlement

of the cladding. As with Zr-alloy cladding, the CRUD should be monitored in plants and be explicitly considered if it is present and modeled as an insulating layer around the fuel rod.

5.2.2.5 Fuel Rod Internal Pressure

There are several possible limits for rod internal pressure that are discussed in the Standard Review Plan Section 4.2. The first and most straightforward is that the rod internal pressure shall not exceed the coolant system pressure. No outward deformation or hydride reorientation is possible if the stress in the cladding is in the compressive directions. This situation does not change with the application of a Cr-coating. Therefore, this limit would still be applicable to Cr-coated Zr cladding.

Greater rod internal pressures may be justified based on the following criteria:

- No cladding liftoff during normal operation
- No reorientation of the hydrides in the radial direction in the cladding
- A description of any additional failures resulting from departure of nucleate boiling (DNB) caused by fuel rod overpressure during transients and postulated accidents.

It has typically been determined by applicants with Zr-alloy cladding that the first of these criteria, no cladding liftoff during normal operation, is the most limiting. This should be confirmed by the applicant of a Cr-coated Zr cladding to still be the case. If this is found to be the case, the pressure limit where cladding liftoff could occur is typically set as the pressure where the upper bound cladding creep rate will exceed the lower bound fuel pellet swelling rate. For Cr-coated Zr cladding, the fuel pellet swelling rate will not be changed and the cladding creep rate will be determined as discussed in Section 5.1.7.

5.2.2.6 Internal Hydriding

Internal hydriding is typically addressed through manufacturing controls on the pellet moisture limit. The inner surface for the Cr-coated Zr cladding will be the same and therefore the typical approach would also apply for Cr-coated Zr cladding. It is not expected that the application of a coating will impact this conclusion.

5.2.2.7 Cladding Collapse

Cladding collapse in modern nuclear fuel rods has been mitigated by pellet design features such as dishes and chamfers on the ends of the pellet that effectively eliminate axial gaps in the fuel pellet column. Nevertheless, cladding collapse analyses are performed for potential small axial gaps between pellets and in the upper plenum region. The key input into this analysis is the cladding creep rate. For Cr-coated Zr the cladding creep rate will be determined as discussed in Section 5.1.7.

5.2.2.8 Overheating of Fuel Pellets

For this analysis, the limit is the melting temperature of the fuel pellets. This will not be impacted by the introduction of Cr-coated Zr cladding and therefore the limit for this SAFDL may stay the same.

5.2.2.9 Pellet-to-Cladding Interaction

Typically, there is no explicit limit set on pellet-to-cladding interaction. Various manufacturing designs and inspections and the transient cladding strain limit are expected to cover this SAFDL. The inner surface for the Cr-coated Zr cladding will be the same and therefore the typical approach would also apply for Cr-coated Zr cladding.

5.2.3 SAFDLs Related to Fuel Rod Performance Assessed for Accident Conditions

Current codes that are informed by the properties in Section 5.1 can perform the following analyses. However, the limits may need revision relative to those typically used for Zr-alloy tubes.

5.2.3.1 Overheating of the Cladding

Overheating of the cladding refers to exceeding the critical heat flux (CHF). Operation above this point results in a reduction of the coolant to remove heat and can result in damage to the cladding. In a PWR, exceeding CHF results in departure from nucleate boiling (DNB). In a BWR, exceeding CHF results in dryout. This thermal margin should not be exceeded for normal operation and AOOs. For design basis accidents the number of fuel rods exceeding thermal margin criteria are assumed to have failed and are included in fission product release dose calculations.

The boiling transitions are shown graphically in Figure 5-1. Typical limits are based on ex-reactor flow tests on electrically heated fuel assembly mockups to determine where CHF occurs. The CHF is primarily influenced on the geometry of the assembly, although surface conditions of the fuel rods may also impact the CHF. Surface conditions include surface roughness, wettability (as indicated by contact angle), and porosity (e.g., of a CRUD layer). Most studies have concluded that roughness has little or no impact on CHF (Collier & Thome, 1994), (Kandlikar, 2001), (O'Hanley, et al., 2013) though some studies have shown a noticeable difference between rough and very smooth surfaces (Weatherford, 1963). Surface porosity and wettability are thought to have a much more significant impact, as demonstrated by several experimental studies (Kandlikar, 2001), (Takata, Hidaka, Masuda, & Ito, 2003), (O'Hanley, et al., 2013).

The application of a coating to fuel rods, while keeping the rest of the assembly the same, is not expected to impact these CHF correlations if the surface conditions of the coating are similar to that of the reference Zr-alloy tubes. It is currently not known what the surface roughness, contact angle, or CRUD deposition rate for a Cr-coated tube will be relative to an uncoated tube. If the coating results in a significantly different surface roughness or cladding outer diameter than the reference Zr-alloy tube, then ex-reactor flow tests on electrically heated fuel assembly mockups with prototypical coated cladding tube could be performed to determine where CHF occurs.

As mentioned in Section 4.1, the possibility of formation of a low temperature eutectic between Cr and Zr exists if temperature exceeds 1332°C. This formation should either be considered under this damage mechanism or under generalized cladding melting (Section 5.2.3.7).

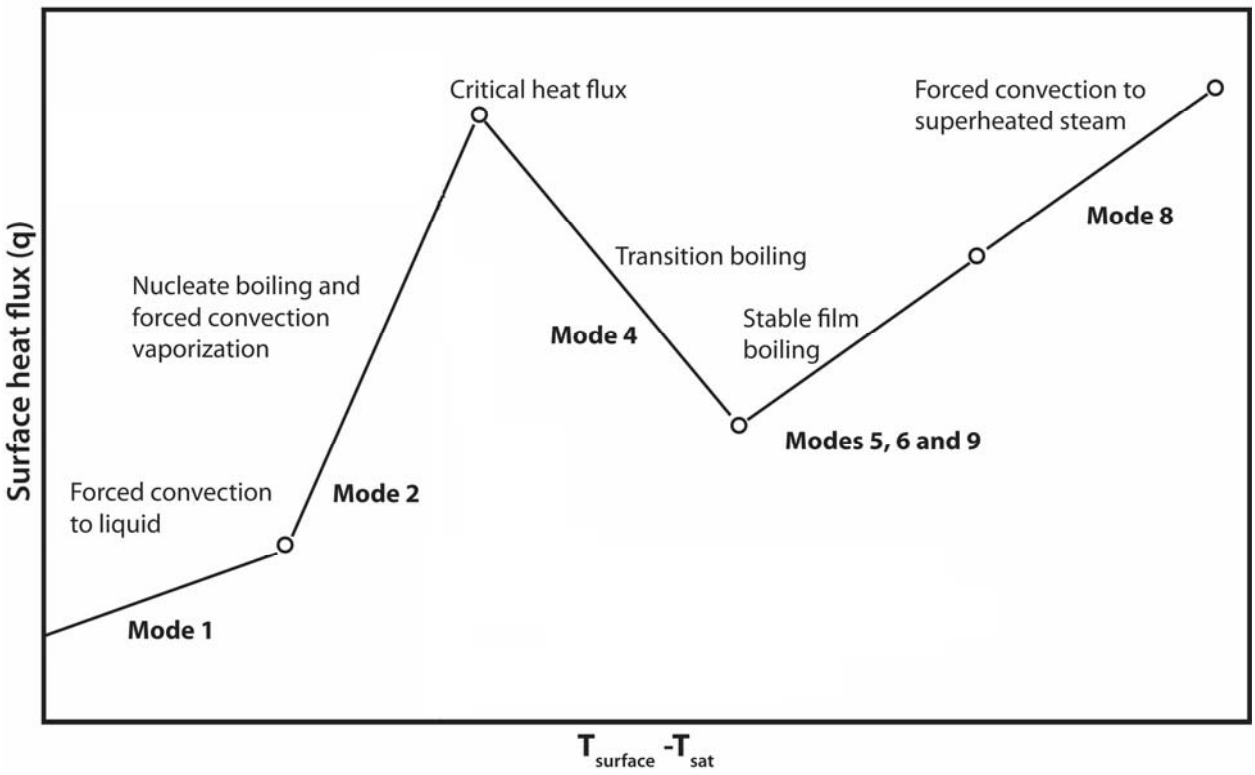

Figure 5-1. Typical boiling transitions

5.2.3.2 Excessive Fuel Enthalpy

Excessive fuel enthalpy relates to the sudden increase in fuel enthalpy from an RIA below the fuel melting limit that can result in cladding failure due to pellet-cladding mechanical interaction. Current fuel enthalpy limits are based on RIA tests that have been performed on irradiated and unirradiated fuel rodlets in various test reactors and a limit has been determined of what level of fuel enthalpy increase will cause cladding failure.

For Zr-alloy cladding, these data have been collected over a very long period and it may not be practical to collect this amount of data for Cr-coated Zr cladding.

An alternate approach comes from the fact that cladding failure due to excessive fuel enthalpy is driven by pellet-cladding mechanical interaction which causes the cladding to exceed its ductility limit. Therefore, it is possible to collect uniform elongation (strain at maximum load) data from the irradiated cladding mechanical tests that need to be performed to collect the elastic modulus (Section 5.1.5) and yield stress data (Section 5.1.6). If it can be shown that the Cr-coating has a beneficial or negligible impact on the uniform elongation relative to the reference Zr-alloy cladding, then it could be reasonably argued that the current RIA failure limits are applicable to Cr-coated Zr cladding. If this were the case then a more limited number of RIA tests on Cr-coated Zr clad fuel rods may be acceptable, or a commitment to collecting such data could be acceptable.

It should be noted that this limit is used to assess the number of fuel rods that are expected to fail during an RIA, and a conservative approach could be taken to either assume all the rods will fail or a

significantly conservative limit could be applied to cover the lack of RIA test data on Cr-coated Zr cladding.

5.2.3.3 Bursting

Bursting of the fuel rod relates to failure of fuel rods due to high temperature and high gas pressures during a LOCA. It is important to know the rupture stress as a function of temperature and the amount of ballooning that would occur. There are no specific design limits associated with cladding rupture other than that the degree of swelling not be underestimated and the balloon not block the coolant channel. Additionally, the time of rupture needs to be known so that oxidation on the cladding inner surface and its associated heat is correctly modeled.

An applicant will typically use an empirical correlation for burst stress and ballooning strain such as the one given in NUREG-0630 (Powers & Meyer, 1980). If an applicant uses NUREG-0630 for Cr-coated Zr cladding, it would be useful to collect some data to show that the performance of Cr-coated Zr is bounded by these limits. Alternatively, if the applicant wants to propose new burst stress and ballooning strain limits, a significant body of burst data would be useful to demonstrate that the degree of swelling not be underestimated. Currently available data suggest that for Cr-coated cladding, the balloon region is smaller and burst temperature increases (see Section 6.2.2), however, this should be confirmed for the specific coating in question.

5.2.3.4 Mechanical Fracturing

Mechanical fracturing refers to a defect in the cladding caused by an externally applied force. Typically, this limit has conservatively been set as applied stresses above 90% of the irradiated yield stress. This limit should not be exceeded for normal operation and AOOs. For design basis accidents the number of fuel rods exceeding this limit are assumed to have failed and are included in fission product release dose calculations.

This limit is acceptable for Cr-coated Zr cladding given that the irradiated yield stress obtained as described in Section 5.1.6 is used.

5.2.3.5 Cladding Embrittlement

Cladding embrittlement relates to embrittlement of the fuel cladding, particularly in the ballooned region of the cladding during LOCA. Cladding embrittlement during LOCA should be precluded so the fuel assemblies with ballooned rods are not severely damaged by post LOCA loads such as reflood and quenching. 10 CFR 50.46 specifies a cladding temperature limit of 2200°F (1204°C) and a peak oxidation of 17% equivalent cladding reacted for Zr-alloy cladding (US Nuclear Regulatory Commission, 2017).

It is not known if these limits will be acceptable for Cr-coated Zr cladding. It appears as if the outer surface will reduce the high temperature metal-water reactor from that of bare Zr, but it is unknown if some other mechanism could cause embrittlement of the cladding. One possible mechanism could be Zr-Cr interdiffusion as discussed in Section 4.2. The formation of a brittle rim of $ZrCr_2$ could lead to brittle cladding failure similar to how the formation of a dense hydride rim can lead to brittle cladding failure.

Tests showing ductility (See Section 6.2.6) at either these existing limits or test establishing new limits would be useful to demonstrate embrittlement will not occur. In addition to the tests performed to establish the ballooning (Section 5.1.11) and high temperature oxidation behavior (Section 5.1.12), some prototypic integral LOCA tests (see for example (Flanagan, Askeljung, & Puranen, 2013)) where cladding tubes are subject to ballooning and burst in steam under expected time frames and samples are then subjected to mechanical loading such as bend tests after ballooning, burst, and high temperature oxidation are very useful to establish cladding embrittlement limits. For these tests, irradiated cladding tubes are preferable.

5.2.3.6 Violent Expulsion of Fuel

Violent expulsion of fuel relates to the sudden increase in fuel enthalpy from an RIA that can result in melting, fragmentation, and dispersal of fuel. This could result in a loss of coolable geometry and produce a pressure pulse that could damage the reactor vessel. Typical limits for violent expulsion of fuel are:

- Peak radial average fuel enthalpy below 230 cal/g
- Peak fuel temperature below melting temperature.

It is expected that cladding failure will occur well before 230 cal/g for both Zr-alloy and Cr-coated Zr cladding. These limits are derived to prevent violent ejection of fuel from failed cladding. As such, these limits relate more to the fuel than to the cladding and are expected to be appropriate for Cr-coated Zr cladding.

5.2.3.7 Generalized Cladding Melting

Generalized cladding melting is applicable to design basis accidents and is set to preclude the loss of coolable geometry. The limit is set as the cladding melting temperature, which for Zr is 1852°C. For Zr-alloy tubes the embrittlement limit of 1204°C (Section 5.2.3.5) is more limiting. However, as discussed in Section 5.2.3.5, it is unknown what the limit for Cr-coated Zr embrittlement will be, so cladding melting should still be considered for Cr-coated Zr.

The melting temperature of Cr (1857°C) is virtually identical to that of Zr (1852°C). However, the formation of a low temperature eutectic between Cr and Zr at 1332°C occurs significantly lower than either of the individual melting temperatures. Formation of a low temperature eutectic with a thin coating may not represent loss of geometry such as generalized cladding melting, but the formation of the eutectic should either be considered under this damage mechanism or under overheating of the cladding (Section 5.2.3.1).

5.2.3.8 Fuel Rod Ballooning

Ballooning of the fuel rod relates to failure of fuel rods due to high temperature and high gas pressures during a LOCA. It is important to know the rupture stress as a function of temperature and the amount of ballooning that would occur. There are no specific design limits associated with cladding rupture other than the degree of swelling not be underestimated and the balloon not block the coolant channel.

An applicant will typically use an empirical correlation for burst stress and ballooning strain such as the one given in NUREG-0630 (Powers & Meyer, 1980). If an applicant uses NUREG-0630 for Cr-coated Zr cladding, it would be useful to collect some data to show that the performance of Cr-coated Zr is bounded by these limits. Alternatively, if the applicant wants to propose new burst stress and ballooning strain limits, a significant body of burst data from either unirradiated or irradiated cladding tubes would be useful to demonstrate that the degree of swelling not be underestimated.

5.2.3.9 Structural Deformation

Structural deformation refers to externally applied loads during LOCA or safe shutdown earthquake that could deform the fuel assemblies or cause fuel fragmentation such that coolable geometry would be lost. This limit has conservatively been set as applied stresses above 90% of the irradiated yield stress. For design basis accidents the number of fuel rods exceeding this limit are assumed to have failed and are included in fission product release dose calculations.

This limit is acceptable for Cr-coated Zr cladding given that the irradiated yield stress obtained as described in Section 5.1.6 is used.

Table 5.3. Tests that could be used to establish SAFDL limits or Cr-coated Zr alloy tubes beyond those needed to quantify basic material properties

SAFDL limit	Recommended Tests
Rod Bow Evaluation	Ensure empirical rod bow method appropriately models LTA rods
Fretting	Ex-reactor tests on unirradiated tubes and grids to demonstrate no damage to either part
Cladding strain/ductility	Ex-reactor tests on irradiated tubes to confirm ductility requirements in strain limits at AOO temperatures
Cladding fatigue	Ex-reactor tests on irradiated tubes to establish fatigue design curve
Thermal limits (DNB, CHF) if surface roughness is different from Zr-alloy tubes	Ex-reactor tests on unirradiated tubes to establish thermal limits (CHF)
Excessive fuel enthalpy	Ex-reactor tests on irradiated tubes to confirm ductility requirements at RIA temperatures RIA tests on irradiated fuel segments in test reactor could be used to develop RIA failure criteria
Cladding Embrittlement	Ex-reactor balloon/burst/bend tests on unirradiated and/or irradiated tubes to confirm existing

	embrittlement limits or develop new embrittlement limits

5.2.4 New Damage Mechanisms

There have been several new damage mechanisms identified for Cr-coated Zr cladding. These may either be addressed by applicants through existing limits or as separate limits. The following sections identify those new damage mechanisms that have been identified for Cr-coated Zr through a technical review of the recent data and a general understanding of coating behavior. Each section will identify the potential for fuel system damage, fuel rod failure, or impact on fuel coolability. These sections will also identify existing SAFDLs that could be used to account for these damage mechanisms.

5.2.4.1 Coating Cracking

Cracking of the coating could occur during the relatively large (0.5% to 1% strain) deformations that are observed occur in the cladding due to cladding thermal expansion, cladding creepdown, and deformation of the cladding due to pellet swelling. Cracking could also occur in the cladding due to repeated small strain (0.01% to 0.1% strain) cyclic operation. Finally, cracking could occur during a design basis accident that causes large strain from pellet expansion (RIA) or gas overpressure and ballooning (LOCA).

Excessive cracking of the coating could eliminate the benefit that the coating provides for normal operation (reduced in-reactor corrosion and hydrogen pickup) as well as during accident conditions (may expose significant amount of Zr to high temperature steam). Cracking of the coating could also create crack tips that extend into the Zr cladding that could provide stress concentrations for further environmentally assisted crack mechanisms and could ultimately lead to cladding failure.

Cracking of the coating should be considered in the development of the cladding strain limit (Section 5.2.2.2) and the cladding fatigue limit (Section 5.2.2.3). In these cases, it should be considered if failure is defined when cracking of the coating is observed. Cracking of the coating should also be considered in the development of high temperature ballooning (Section 5.1.11) and high temperature oxidation (Section 5.1.12) correlations. If cracking is observed following ballooning, then high temperature oxidation correlations should be developed based on cladding with a cracked coating. Additionally, cladding embrittlement limits (Section 5.2.3.5) should be developed based on cracked cladding.

5.2.4.2 Coating Delamination

Delamination of the coating could occur due to a variety of reasons including poor adherence to the substrate and differential thermal expansion between the coating and the substrate.

Delamination of the coating could eliminate the benefit that the coating provides for normal operation (reduced in-reactor corrosion and hydrogen pickup) as well as during accident conditions (may expose significant amount of Zr to high temperature steam) depending on the amount of delamination. Local coating delamination could create a local cool spot on the cladding which is a sink for hydrogen diffusion. This local cool spot could develop a hydride blister that results in local brittle cladding behavior. Finally, coating delamination can increase the quantity of debris in the reactor coolant system which could lead to enhanced debris fretting and could impact the performance of emergency core coolant system pump in the

event of an accident if the debris filters become clogged with debris from delaminated coating. Debris clogging this pump has been identified as Generic Safety Issue 191 (GSI-191) (Shaffer, et al., 2005).

Delamination of the coating should be considered in the development of the cladding strain limit (Section 5.2.2.2) and the cladding fatigue limit (Section 5.2.2.3). In these cases, it should be considered if failure is defined to be observed delamination of the coating. Delamination of the coating should also be considered in the development of high temperature ballooning (Section 5.1.11) and high temperature oxidation (Section 5.1.12) correlations. If delamination is observed following ballooning, then high temperature oxidation correlations should be developed based on cladding with a delaminated coating. As discussed in Section 4.2, the $ZrCr_2$ phase that could form due to interdiffusion could exhibit greater corrosion rate than bare Zr. Additionally, if this is the case, cladding embrittlement limits (Section 5.2.3.5) should be developed based on delaminated cladding. To address GSI-191, the potential for delamination should be evaluated and accounted for following burst (Section 5.2.3.3), mechanical fracture (Section 5.2.3.4), ballooning (Section 5.2.3.8), and structural deformation (Section 5.2.3.9).

5.2.4.3 Cr-Zr Interdiffusion

As discussed in Section 4.2, if temperatures at the Cr-Zr interface and the time at temperature are great enough there will be the formation of a CrZr intermetallic that is more brittle than either Cr or Zr separately. The calculations from Section 4.2 are shown below.

- Normal Conditions (300°C-350°C for 2000 days) 0.1 to 0.3 μm thick intermetallic layer
- Loss-of-coolant Conditions (800 to 1200°C for 1 hour) 0.2 to 1.4 μm thick intermetallic layer
- Long term Loss-of Coolant (800 to 1200°C for 1 day) 1 to 7 μm thick intermetallic layer.

Unless otherwise accounted for in specific strain or ballooning limits, the formation of this CrZr intermetallic should be avoided. During normal operations and AOOs, the temperature at the Cr/Zr interface is only expected to allow for the formation of a very thin CrZr intermetallic layer, but during design basis accidents the cladding temperature may be large enough to form a significant thickness of this layer (See Section 4.2). Other possibilities for the formation of the CrZr intermetallic phase include during application of the coating if the substrate temperature is too great, and during the welding of end caps in the heat affected zone of the weld.

The Cr/Zr intermetallic is both brittle and exhibits extremely poor high temperature corrosion behavior (See Section 4.2). If a significant thickness of Cr/Zr intermetallic were to form during high temperature conditions during a design basis accident or some manufacturing process, the cladding could behave in a brittle manner, the corrosion reaction may worsen, and various design limits on strain and cladding embrittlement may no longer be applicable.

Cr-Zr interdiffusion should be considered in the development of limits on overheating of the cladding (Section 5.2.3.1), clad embrittlement (Section 5.2.3.5), and eutectic formation related to generalized clad melting (Section 5.2.3.7). If some Cr-Zr interdiffusion is caused during the manufacturing process, then it should be ensured that limits are developed on prototypic parts from this process and tests are performed in localized areas known to have the possibility for interdiffusion.

5.2.4.4 Radiation Effects on Cr

It has been noted that the irradiation of Cr will result in the formation of the radioisotope Cr-51 with a half-life of 28 days. It is known that this isotope will be formed, but it is not known if this isotope will be released to the coolant in significant quantities. A second concern is what the impact of fast neutron irradiation on Cr metal and other Cr containing compounds will be. In zirconium, fast neutron irradiation leads to a dramatic increase in strength and reduction in ductility (Geelhood, Beyer, & Luscher, 2008).

The release of Cr-51 from the cladding into the coolant could challenge the plant dose release limit or the ability of the chemical and volume control system to eliminate Cr ions before they plate out on the fuel and the other reactor components. The impact of fast neutron irradiation on the strength and ductility of the Cr metal or other Cr containing compounds could lead to a degradation in coating performance beyond what we expected based on tests on unirradiated material.

The formation and possible release of Cr-51 is an issue that may be monitored through ongoing surveillance at the plant. Plants already have a process in place to evaluate the radioisotopes and the gaseous and liquid effluents and report this information to the NRC on an annual basis. If Cr-51 in the coolant begins to challenge plant dose release limits, it will be observed to increase as more of the fuel in the core is transitioned to Cr-coated Zr cladding. In this case, systems can be implemented to effectively remove this radioisotope before it becomes a safety problem. Similarly, with the impact of Cr ions on the coolant chemistry, a surveillance plan put in place alongside the implementation of Cr-coated Zr cladding to monitor the coolant chemistry will mitigate any impact of Cr ions. The impact of fast neutron irradiation on Cr mechanical properties will be inherently included in material property correlations and limits that are developed based on irradiated material as described in previous sections.

5.3 Changes to Existing Codes and Methodologies

This section discusses the changes to existing codes and methodologies.

5.3.1 Codes

As mentioned at the beginning of Section 5.0 there are two basic approaches that an applicant could use during the update of their codes and methods for Cr-coated cladding. They could attempt to treat the cladding and the coating separately, which would require correctly modeling the interface for thermal and mechanical analyses, or they could treat the coated cladding as a single material with effective mechanical and thermal properties. The first approach would require the applicant to modify their codes to include the effect of the material interfaces as well as include material properties for the coating material. The second approach would only require the applicant to include the material properties discussed in Section 5.1 into their code. This approach could also attempt to make an argument to ignore the coating in the analyses and rely on existing cladding properties.

The critical need for the updated codes, regardless of the approach that is taken, is validation. Validation of a computer code is typically performed on five areas that directly relate to various SAFDLs. These are also the areas used to assess FRAPCON (Geelhood & Luscher, 2015)

- Fuel temperature

- Fission gas release
- Rod internal pressure and void volume
- Cladding oxide thickness
- Cladding permanent hoop strain following a power ramp.

If it is determined that the coating has an impact on the CHF correlations, then some testing should also be performed to determine the CHF correlation for the coated cladding for subchannel or systems analysis codes.

Details for each of these assessments is discussed in the following sections as they relate to the assessment of a code to correctly model Cr-coated Zr cladding. Table 5.4. provides test data that could be used in code assessment.

5.3.1.1 Fuel Temperature

A fuel thermal mechanical code will be used to assess the power to melt limit as well as provide initial conditions to accident analyses. It is noted that the introduction of a Cr-coated Zr cladding will likely have minimal impact on the predicted temperatures in the fuel. The coating is very thin and should offer minimal temperature change across its thickness or the thickness of the Cr_2O_3 that develops. Additionally, it is expected that the cladding mechanical behavior of the Cr-coated Zr should be similar to that of Zr-alloy cladding that have been successfully modeled. Temperature data was historically collected in the Halden Reactor in Norway, which has recently been permanently shut down. Other reactor capabilities are being examined to determine how this capability can be replaced. Given that this change is only to the cladding and if cladding properties are correctly implemented into a fuel thermal mechanical code, it is reasonable to assume that the previous assessment on Zr-alloy clad UO_2 will be acceptable for Cr-coated Zr clad UO_2.

5.3.1.2 Fission Gas Release

Fission gas release is primarily driven by fuel temperature, time, and power level. Fission gas release can drive fuel temperatures and rod internal pressure, and as such is a key metric of success in a fuel thermal mechanical code. As mentioned in the previous section the fuel temperature should be adequately predicted by a validated fuel code, so the fission gas release should also be adequately predicted.

Any fission gas release from destructive examination of LTAs, particularly high-power LTAs would be useful in the assessment of a thermal mechanical code used for safety analysis of Cr-coated Zr cladding. An ongoing surveillance plan with the goal of continuing to obtain more fission gas release data would provide additional assessment data.

5.3.1.3 Rod Internal Pressure and Void Volume

A fuel thermal mechanical code will be used to assess the rod internal pressure relative to the pressure limit that has been derived by the applicant. Void volume is impacted by component temperatures and deformations and in the case of Cr-coated Zr could be impacted if the Cr-coated Zr had a significantly

different creep rate than Zr-alloy cladding. The rod internal pressure is driven primarily by the void volume, fission gas release and component temperature and therefore could also be impacted.

Any void volume and rod internal pressure from destructive examination of LTAs, particularly high-power LTAs, would be useful in the assessment of a thermal mechanical code used for safety analysis of Cr-coated Zr cladding. An ongoing surveillance plan with the goal of continuing to obtain more void volume and rod internal pressure data would provide additional assessment data.

5.3.1.4 Cladding Oxide Thickness

Cladding oxide thickness is important because it can have a feedback on the fuel and cladding temperature predictions. Additionally, a fuel performance code will be used to assess the cladding oxide thickness relative to limits derived by the applicant. The data used to develop the cladding oxidation rate discussed in Section 5.1.9 is the same data that would be used to assess the code's prediction of oxidation rate. There is no additional requirement on validation beyond this. However, it should be noted that due to potential issues with coating cracking and spallation, a surveillance plan to monitor the oxide thickness on Cr-coated Zr cladding would be useful as it may give an early indication of a process change that is causing a problem.

5.3.1.5 Cladding Permanent Hoop Strain Following a Power Ramp

A fuel thermal mechanical code will be used to assess the cladding permanent hoop strain during an AOO power ramp to compare to the cladding strain limit. It is noted that the introduction of a Cr-coated Zr cladding may not have a significant impact on the predicted permanent hoop strain following a power ramp depending on how close the creep and elastic properties of Cr-coated Zr cladding are to Zr-alloy cladding. Nevertheless, power ramp tests on rodlets refabricated from irradiated fuel rods would be helpful to assess the code prediction of hoop strain following a power ramp. If it can be demonstrated that the impact of the Cr-coating is minimal or can be accounted for with the code and associated uncertainties, then it could be acceptable to use a relatively small database of ramp tests to assess the code's prediction in this area.

Table 5.4. Assessment data that could be used to validate fuel thermal mechanical codes for Cr-coated Zr alloy tubes

Assessment Data	Recommended Tests
Fuel centerline temperature	Any that can be obtained, but not critical
Fission gas release	LTA data and follow-up surveillance plan
Rod internal pressure and void volume	LTA data and follow-up surveillance plan
Cladding oxide thickness	Initially none beyond data in Table 5.1. and follow-up surveillance plan
Cladding permanent hoop strain	Power ramp tests to assess the prediction of cladding strain following power ramp

5.3.2 Methodologies

The methodology for performing the fuel system safety analysis consists of the following pieces:

- Identification of functional requirements for the fuel and assembly
- Identification of limits for each functional requirement
- Identification of code or other approach that will be used to assess performance against functional requirement
- Identification of approach to demonstrate high level of confidence that design will not exceed functional requirements:
  - Selection of power histories to be considered
  - Identification of uncertainties in operational parameters
  - Identification of fabrication uncertainties
  - Identification of modeling uncertainties
  - Approach to quantify an upper tolerance level based on identified uncertainties.

The identification of functional requirements for the fuel and assembly and the limits for each are discussed in Section 5.2. There have been new damage mechanisms identified in Section 5.2.4 that should be implicitly handled via existing SAFDLs and considered in the development of those SAFDL limits. Alternatively, the methodology may be modified to explicitly address these mechanisms through new functional requirements and limits.

The material property updates and the code assessment has been discussed in Sections 5.1 and 5.3.1. No further methodology change is anticipated as far as the use of codes is considered.

The identification of operational parameters such as rod power, coolant flow rate, etc. are not expected to be impacted by the implementation of Cr-coated Zr cladding.

The identification of fabrication uncertainties will be taken from uncertainty specifications on the drawings or from manufacturing data. Although specific values may change, the general approach for obtaining these values is not expected to change.

The identification of modeling uncertainties should be developed during the implementation of new material properties and code assessment. Comparing property data to correlations and code predictions to measurements should allow for the appropriate development of acceptable modeling uncertainties.

Existing approaches to calculate upper tolerance levels are robust and should be acceptable to perform these calculations for Cr-coated Zr cladding given that the activities discussed above are rigorously performed.

6.0 Currently Available Data

This section describes the data that are currently available on Cr-coated Zr cladding including coatings of Cr, Cr-alloys, CrN, and GNF ARMOR coatings. The presence of data in any area does not indicate that an applicant would not have to provide data from their specific coated cladding because it has been observed that coating processes and other processes can impact the performance of the cladding and the coatings. Rather these data are compiled here to give the NRC staff expected performance of coated cladding as well as areas of concern that should be given additional scrutiny during the review of one of these concepts.

The data historically provided for qualification of new Zr-alloy cladding are listed in Table 5.1., Table 5.3, and Table 5.4.. These data can be grouped into 1) data that need to be collected in-reactor or during a poolside examination or post-irradiation examination, 2) data that may be collected on unirradiated cladding samples, and 3) data that must be collected on previously irradiated cladding samples. The data or lack of data in each of these categories is discussed in the following sections.

6.1 In-Reactor Data

Recommended qualification data from an in-reactor test program are:

- Thermal and irradiation creep behavior
- Axial irradiation growth
- Oxidation rate
- Hydrogen pickup
- Rod bow evaluation
- RIA test
- Fuel centerline temperature
- Fission gas release
- Rod internal pressure and void volume
- Cladding permanent hoop strain following a power ramp.

6.1.1 Current Irradiation Tests

ATR ATF-1 Test

The advanced test reactor at Idaho National Laboratory (INL) conducted the ATF-1 irradiation test on a number of different ATF concepts. There were no Cr-coated Zr cladding samples irradiated in this test. (Core, 2016) (Harp & Cappia, 2019).

Halden IFA-774 Test

Test rods clad in Zr coated in CrN, AlCrN, and TiAlN were irradiated in the Halden Reactor in IFA-774 to a low burnup level of 6.5 MWd/kgUO_2. (Anderson & Van Nieuwenhove, 2016) (Van Nieuwenhove, 2014) A mechanical deformation in the rig structure gave reason to assume that the cooling of the rods was not sufficient, and that local overheating of the fuel rod claddings occurred. It is not known when the deformation occurred; hence it is not known for how long the coolant flow might have been affected. Neither the TiAlN nor the AlCrN coating survived the test. The CrN coating performed better but displayed cracking and missing parts with about 80% of the coating remaining.

Halden IFA-796 Test

Test rods clad in Zr coated with Cr provided by Westinghouse and Framatome and Zr coated with CrAl provided by KAERI were irradiated in the Halden Reactor in IFA-796 (Szoke & Bennett, 2017). Plans were to irradiate these rods to 40 MWd/kg UO_2 but the shutdown of the Halden Reactor resulted in only one cycle of irradiation to about 55 days. Visual examination of the rods has been completed. Destructive post irradiation examination has not yet begun.

Gösgen IMAGO Program

Unfueled Cr-coated Zr rods provided by Framatome are being irradiated in the Gösgen nuclear power plant in Switzerland since 2016 (Girardin, et al., 2018). These tubes are planned to be irradiated until 2023, although some samples may be extracted at various times. These tubes will provide irradiated material for future test samples. It should be noted that because these samples did not contain fuel or have prototypical surface heat flux, these samples will have limited value for determining oxide thickness but will be useful for measuring mechanical properties.

MITR MITR-2 Test

Unfueled Cr-coated Zr rods provided by Westinghouse have been irradiated in the MITR test reactor for 157 days (Xu, et al., 2017). Visual examination, weight gain, and microstructure of the cladding tubes were observed.

Lead Test Rod Irradiation Programs

US fuel vendors are currently engaging in lead test rod irradiation programs. In these programs a limited number of ATF rods are being irradiated by replacing standard fuel rods in one or more fuel assemblies.

Framatome is planning a lead test rod irradiation of Cr-coated M5® in the Vogtle and ANO nuclear power plants starting in 2019 (Bischoff, et al., 2018).

Westinghouse is planning a lead test rod irradiation of Cr-Coated ZIRLO with U_3Si_2 fuel and doped UO_2 (ADOPT™) fuel in the Byron nuclear power plant staring in 2019 (Shah, et al., 2018).

GNF has been irradiating lead test rod of Coated Zr clad (ARMOR) with UO_2 fuel in the Hatch nuclear power plant since spring of 2018. The first poolside examination is planned for 2020 (Lin, et al., 2018).

6.1.2 Planned Irradiation Tests

The following items describe irradiation tests on Cr-Coated Zr cladding concepts that are being planned for the near future.

ATR ATF-2 Test

Rodlets provided by Framatome with Cr-coated M5® and Cr_2O_3 doped UO_2 and rodlets provided by Westinghouse with Cr-coated ZIRLO and UO_2 are planned to be irradiated in the ATR test reactor. Irradiation is planned in a flowing water loop. Plans are to install instrumentation to measure irradiation temperature, neutron flux, fuel and cladding dimensional changes, and rod internal pressure (Idaho National Laboratory, 2018).

MITR MITR-3 Test

Plans are underway to irradiate tubes of Cr-coated ZIRLO provided by Westinghouse in the MITR test reactor. The details of this test are not available, and it is unknown how this test will be different from the MITR-2 test already performed (Xu, et al., 2017).

HFIR at ORNL

Plans are underway to irradiate Cr-coated M5® for Framatome and ARMOR-coated Zircaloy-2 for GNF in the HFIR reactor at Oak Ridge National Laboratory (ORNL). The samples are planned to be un-fueled cladding segments focused on measurements of the cladding properties under irradiation.

6.1.3 Recommended Irradiation Tests

Irradiation test data for Cr-coated Zr cladding is relatively sparse, but several irradiation tests are underway or are about to begin. Table 6.1. provides the in-reactor test data is recommended for fuel qualification and an indication of where these data may be obtained or in some cases indicate an irradiation test that is necessary. Current irradiation data and planned irradiation tests do not address the collection of irradiation creep data or power ramp data. Additionally, RIA tests have not been identified.

Table 6.1. Fuel qualification data recommended from in-reactor tests for Cr-coated Zr alloy tubes

Data	Possible source of data
Thermal and irradiation creep behavior	In-reactor pressurized cladding tube creep tests – no current plans. Note some creep data could be obtained from LTAs prior to fuel/clad gap closure.
Axial irradiation growth	Poolside examination of lead test rods
Oxidation rate	Poolside examination of lead test rods
Hydrogen pickup	Post irradiation examination of lead test rods

Rod bow evaluation	Poolside examination of lead test rods
RIA test	RIA test in a reactor such as NSRR on segment refabricated possibly from lead test rod – no current plans, but may not be necessary
Fuel centerline temperature	Possibly obtained from ATF-2 test in ATR – may not be necessary
Fission gas release	Post irradiation examination of lead test rods
Rod internal pressure and void volume	Post irradiation examination of lead test rods
Cladding permanent hoop strain following a power ramp	Ramp test in a test reactor refabricated possibly from lead test rod – no known plans

6.2 Ex-Reactor Data Collected on Unirradiated Samples

Recommended qualification data from ex-reactor tests on unirradiated samples are:

- Thermal conductivity
- Thermal expansion
- Specific heat and enthalpy
- Ballooning
- High temperature corrosion
- Fretting
- Thermal limits (DNB, CHF)
- LOCA post quench ductility.

The following will describe the data that are available with overall observations from data that are available.

6.2.1 Thermal Properties

No data has been found in the literature from Cr-coated Zr cladding for thermal conductivity, thermal expansion, or specific heat and enthalpy.

6.2.2 Ballooning

Framatome has published some ballooning data that shows ballooning during a temperature ramp and other data that shows ballooning at constant temperature and pressure (creep). The results are summarized in Table 6.2. In general, the results indicate at least for the Framatome material, reduced ballooning strain, and increased time and temperature to rupture for Cr-coated Zr cladding relative to uncoated cladding.

Table 6.2. Summary of ballooning data for Cr-coated Zr cladding

Organization	Cladding	Test Description	Results
Framatome (Dumerval, et al., 2018)	Cr-coated M5® by PVD	Temperature ramps on pressurized tube to rupture	Ballooning strain in coated tubes 10-20% strain less than uncoated tubes. Burst temperature about 50°C greater in coated tubes than uncoated tubes
Framatome (Delafoy, et al., 2018)	Cr-coated M5® by PVD	Constant temperature and pressure. Measure time to rupture	Failure times in coated tubes 2 to 3 times greater than uncoated tubes Significant reduction in balloon size in coated tubes relative to uncoated tubes
Framatome (Brachet, et al., 2017)	Cr-coated M5® by PVD	Temperature ramps on pressurized tube to rupture Constant temperature and pressure. Measure time to rupture	Creep time to rupture 2 to 5 times greater than uncoated tubes Significant reduction in balloon size in coated tubes relative to uncoated tubes

6.2.3 High Temperature Corrosion

Significant data exists in the literature on the high temperature corrosion rate of unirradiated Cr-coated Zr, CrN-coated Zr and ARMOR-coated Zr between 800°C and 1500°C. These data are summarized in Table 6.3.. In general, all these coatings have been found to provide improved corrosion resistance relative to Zr-alloy cladding. Framatome and Westinghouse tested samples beyond the eutectic point at 1332°C.

Above the eutectic point, localized melting was observed, but gross cladding failure was not observed which would indicate at least some benefit to the Cr-coating above 1332°C. Another researcher tested uncoated Zr, Cr-coated Zr, and Cr metal in 1200°C steam and found that while the Cr-coated Zr provided improved corrosion resistance relative to the uncoated Zr, it did not perform as well as the Cr metal. The Cr-coated rods were previously subjected to pressurization and depressurization cycles that may have resulted in cracks in the Cr-coating that reduced the oxidation resistance.

Table 6.3. Summary of high temperature oxidation data for Cr-coated Zr cladding

Organization	Cladding	Test Description	Results
Various Chinese state organizations (Wang, et al., 2018) (Liu, et al., 2018)	Cr-coated Zry-4 by plasma spray	1200°C steam for 1 hour	Weight gain of coated sample about half uncoated sample
Framatome (Bischoff, et al., 2018)	Cr-coated M5® by PVD	Ramp test beyond eutectic to 1500°C	Evidence of localized melting but sample retained it integrity and geometry
Framatome (Brachet, et al., 2018)	Cr-coated M5® by PVD	Steam between 1000°C and 1500°C	Significant reduction in oxidation rate of coated samples relative to uncoated samples Above 1350°C formation of eutectic caused surface blisters
Framatome (Bischoff, et al., 2018)	Cr-coated M5® by PVD	Steam at 1100°C	Weight gain of coated samples about 10 times lower than uncoated samples
Framatome (Brachet, et al., 2017)	Cr-coated M5® by PVD	Steam at 1200°C	Weight gain of coated samples about 10 times lower than uncoated samples
GNF (Lin, et al., 2018)	ARMOR-coated Zry-2	Steam at 1000°C	Coated surface had significantly less oxidation than uncoated surface
Halden (Van Nieuwenhove, 2014)	CrN, TiAlN, and ZrO_2 coated Zry	Steam at 1100°C for 15 minutes	TiAlN, and ZrO_2 coatings disappeared. CrN

			survived with no reduction in thickness, cracks or pores
KAERI (Kim, et al., 2015)	Cr-coated Zry-4 by 3D laser coating	Steam at 1200°C for 20 minutes	Oxide layer thickness was 25 times lower on coated cladding than uncoated cladding
CEA, University of Paris (Michau, et al., 2018)	Cr-coated Zry-4 by CVD	1200°C in air	Weight gain was 4 times lower for coated cladding than uncoated cladding
MIT (Sevecek, et al., 2018)	Cr-coated Zry-4 by cold spray & pure Cr metal	1200°C steam	Weight gain 6 times lower for coated cladding than uncoated cladding. Weight gain of Cr metal 200 times lower than uncoated Zircaloy.
MIT (Shahin, Petrik, Seshadri, Phillips, & Shirvan, 2018)	Cr-coated Zry-4 by cold spray	1200°C steam	Oxide thickness 2 times lower on coated cladding than uncoated cladding
Czech Technical Institute (Krejci, et al., 2018)	Cr and CrN layers on E110	1200°C steam	Lower oxide thickness (about a factor of 5) in coated cladding than expected for uncoated cladding
Westinghouse (Oelrick, Xu, Lahoda, & Deck, 2018)	Cr-coated ZIRLO by cold spray	1300°C steam for 5 minutes	Little oxidation on coated cladding in comparison to uncoated cladding
Westinghouse (Oelrich, et al., 2018)	Cr-coated ZIRLO by cold spray	1300°C and 1500°C steam for 5-25 minutes	No significant weight gain at 1300°C, Evidence of surface melting seen at 1500°C

6.2.4 Fretting

Several fretting tests have been performed and indicate that Cr-coated and ARMOR-coated Zr exhibits superior wear resistance relative to uncoated Zr. These data are summarized in Table 6.4.. No data have been provided to explicitly show the impact of wear on grid components from the hard coatings that have been applied to the cladding tubes, however, some of the wear tests were performed with grid components.

Table 6.4. Summary of fretting data for Cr-coated Zr cladding

Organization	Cladding	Test Description	Results
Framatome (Bischoff, et al., 2018)	Cr-coated M5® by PVD	300°C water with PWR chemistry. 100 hours at 20 Hz. Wear from grid components	Wear depth 5 times lower for coated cladding than for uncoated cladding
Framatome (Delafoy, et al., 2018)	Cr-coated M5® by PVD	300°C water with PWR chemistry. Wear from grid components and from AISI wire	Wear depth 10 times lower for coated cladding than for uncoated cladding
Framatome (Bischoff, et al., 2018)	Cr-coated M5® by PVD	300°C water with PWR chemistry. Wear from stainless steel wire to simulate debris fretting	Wear depth 2 times lower for coated cladding than for uncoated cladding
Framatome (Brachet, et al., 2017)	Cr-coated M5® by PVD	300°C water with PWR chemistry. Wear from grid components	Wear depth 10 times lower for coated cladding than for uncoated cladding
GNF (Lin, et al., 2018)	ARMOR-coated Zry-2	Room temperature air with stainless steel wires	Wear depth 3 times lower for coated cladding than for uncoated cladding

6.2.5 Thermal Limits

No data has been found in the literature from Cr-coated Zr cladding for different thermal limits. It is noted however, that most of the coatings that have been developed to date have a fine surface finish, so it is not expected that the boiling behavior would change as a result of adding any of the Cr-coatings.

6.2.6 LOCA Post Quench Ductility

Several tests have been performed to measure the LOCA post quench ductility of Cr-coated Zr cladding. These data are summarized in Table 6.5.. Cr and CrN coatings increase the time at temperature prior to cladding embrittlement. However, it is also clear that embrittlement does eventually occur and current LOCA limits (1204°C and 17% ECR) will **not** protect the cladding from embrittlement. The current LOCA limits are designed to protect against hydride embrittlement. However, the following data show embrittlement after time at 1200°C and only 3-5% ECR and very little hydrogen content. Clearly some other mechanism is causing embrittlement in these samples. As discussed in Section 5.2.3.5 new embrittlement limits are likely required for Cr-coated Zr cladding.

Table 6.5. Summary of LOCA post quench ductility data for Cr-coated Zr cladding

Organization	Cladding	Test Description	Results
Framatome (Brachet, et al., 2018)	Cr-coated M5® by PVD	Ring compression tests following one-sided oxidation at 1200°C	Increase in time at 1200°C before post-quench embrittlement in coated cladding relative to uncoated cladding
Framatome (Brachet, et al., 2017)	Cr-coated M5® by PVD	Direct water quenching following one-sided oxidation at 1200°C	Factor of 2 delay in time of multi-fragmentation of tube upon quenching
KAERI (Park, et al., 2016)	Cr-coated Zr alloy by cold spray	Heating to 1200°C, 300s at 1200°C, cooled to 800°C, quenched with water, 4-point bend	Somewhat greater ductility for coated sample than for the uncoated sample
KAERI (Kim, et al., 2018)	CrAl-coated Zry-4 by 3D laser printing	Heating to 1200°C, 3000s at 1200°C, cooled to 800°C, quenched with water,	Coated cladding remained without damage while uncoated cladding was damaged severely by thermal shock
Czech Technical Institute (Krejci, et al., 2018)	Cr and CrN layers on E110	Oxidation at 1200°C, ring compression tests at 135°C	Evidence of increase in time to ductility reduction. However, embrittlement is seen at very low weight gains (3-5% ECR). Not caused by hydrogen (120 ppm)

6.2.7 Other Data

Numerous autoclave tests have been performed on Cr-coated Zr, CrN-coated Zr, and ARMOR-coated Zr in water and steam between 360°C and 520°C. These data are summarized in Table 6.6.. Typically, the coated cladding samples exhibit improved corrosion resistance relative to uncoated cladding samples. Autoclave tests are useful for screening new materials and indicating if one material will have improved corrosion resistance relative to another. However, in-reactor corrosion rates should not be deduced from autoclave test data (Cox, 2005) (Sabol, Comstock, Weiner, Larouere, & Stanutz, 1993) (Garde, Pati, Krammen, Smith, & Endter, 1993). As previously discussed (Section 5.1.9) these rates should be obtained from in-reactor measurements from fueled rods at typical power levels in prototypical coolant conditions.

Table 6.6. Summary of autoclave corrosion data Cr-coated Zr cladding

Organization	Cladding	Test Description	Results
Various Chinese state organizations (Liu, et al., 2018)	Cr and CrN, and CrAl - coated Zr by PVD	360°C for 72 hrs	Corrosion of all coated tubes a factor of 2-3 lower than uncoated tubes
Framatome (Bischoff, et al., 2018)	Cr-coated M5® by PVD	360°C for 170 days	No breakaway observed for coated cladding after 170 days. Breakaway for uncoated cladding observed after 140 days
Framatome	Cr-coated M5® by PVD	360°C water for 240 days and 415°C steam for 100 days	In 360°C water weight gain about 30 times lower for coated cladding than uncoated cladding In 415°C steam oxide thickness was 100 times lower for coated cladding than uncoated cladding
GNF (Lin, et al., 2018)	ARMOR-coated Zry-2	400°C and 520°C steam	No oxide visually observed on coated cladding. Weight gain about a factor of 8 lower for coated cladding than for uncoated cladding
Halden (Van Nieuwenhove, 2014)	CrN, TiAlN, and ZrO_2 coated Zry	650°C water	TiAlN coating disappeared. ZrO_2 coating had reduced thickness. CrN survived with no reduction in thickness, cracks or pores
KAERI (Kim, et al., 2018)	CrAl-coated Zry-4 by arc ion plating	360°C water 240 days	Weight gain about 2 times lower for coated cladding than uncoated cladding
MIT (Sevecek, et al., 2018)	Cr-coated Zry-4 by cold spray & pure Cr metal	500°C steam 20 days	Weight gain 6 times lower for coated cladding than uncoated cladding. Weight gain of Cr metal 200 times lower than uncoated Zircaloy.

Czech Technical Institute (Krejci, et al., 2018)	Cr-coating on E110	360°C water 210 days	Weight gain 8 times lower for Cr coated cladding than uncoated cladding
Westinghouse (Xu, et al., 2017)	Cr-coating on ZIRLO by cold spray	360°C water 20 days	Visual only

Framatome provided some weld qualification data that indicated the microstructure around the heat affected zone of the weld. These data are summarized in Table 6.7.

Table 6.7. Summary of weld qualification data Cr-coated Zr cladding

Organization	Cladding	Test Description	Results
Framatome (Brachet, et al., 2017)	Cr-coated M5® by PVD	Cr-coating was removed 10 mm from weld	Electron beam welding successful
Framatome (Bischoff, et al., 2018)	Cr-coated M5® by PVD	Welding and ASTM G2 corrosion tests in 360°C water and burst tests	Current resistance welding process successful with no modifications to parameters. Burst occurred outside weld region.

GNF provided some data to indicate ARMOR and coatings were adherent under thermal cycling. KAERI provided some data to indicate cracking of Cr-coating were not observed until greater than 4% strain. These data are summarized in Table 6.8.

Table 6.8. Summary of coating adherence for Cr-coated Zr cladding

Organization	Cladding	Test Description	Results
GNF (Lin, et al., 2018)	ARMOR-coated Zry-2	Repeated thermal cycling to 350°C followed by water quench	No cracking or delamination of the coating
KAERI (Kim, et al., 2015)	Cr-coated Zry-4 by 3D laser coating	Ring compression and ring tensile tests	No cracks in coating observed at 2% or 4% strain. Cracks observed at 6% strain

6.3 Ex-Reactor Data Collected on Irradiated Samples

Recommended qualification data from ex-reactor tests on irradiated samples are:

- Elastic modulus
- Yield stress
- Uniform elongation/ductility (normal operation and AOO)
- Uniform elongation/ductility (RIA)
- Fatigue.

The following will describe the data that are available with overall observations from data that are available.

6.3.1 Mechanical Properties

No data showing irradiated mechanical properties of Cr-coated Zr cladding has been found (elastic modulus, yield stress, and uniform elongation). Several sources of unirradiated mechanical properties of Cr-coated Zr have been found. The data are summarized in Table 6.9.. In general, the results indicate that, in unirradiated conditions, the mechanical properties at room temperature and normal operating conditions are effectively not impacted by the application of a coating. The data also show that, in the unirradiated conditions, the coating can survive without crack significantly beyond 1% hoop strain. Irradiation causes a drastic increase in strength and decrease in ductility in Zr-alloys (Geelhood, Beyer, & Luscher, 2008). For this reason, the impact of the Cr-coatings on the mechanical properties (elastic modulus, yield stress, and ductility) will need to be quantified with irradiated cladding data.

Table 6.9. Summary of unirradiated mechanical properties data for Cr-coated Zr cladding

Organization	Cladding	Test Description	Results
Framatome (Brachet, et al., 2017)	Cr-coated M5® by PVD	Tensile tests at room temperature and 400°C Thermal creep at 400°C for 240 hours	Elastic modulus, yield stress, ultimate tensile strength and uniform elongation similar for coated and uncoated cladding. Thermal creep similar for coated and uncoated cladding
KAERI (Kim, et al., 2015)	Cr-coated Zry-4 by 3D laser coating	Ring tensile and ring compression tests	Elastic modulus, yield stress, ultimate tensile strength and uniform elongation similar for

			coated and uncoated cladding. No cracking observed at 2% or 4% hoop strain. Cracking observed at 6% strain
MIT (Shahin, Petrik, Seshadri, Phillips, & Shirvan, 2018)	Cr-coated Zry-4 by cold spray	Burst test at room temperature	Ultimate tensile strength, burst pressure, and burst strain about the same for coated and uncoated cladding

6.3.2 Fatigue

There is little fatigue data for Cr-coated Zr. The data that does exist is for unirradiated Cr-coated Zr. The data are summarized in Table 6.10.. For Zr-alloy cladding the fatigue life has been shown to decrease with irradiation (O'Donnell & Langer, 1964). The available data indicates that fatigue failure occurs significantly earlier in Cr-coated samples than in uncoated samples. The authors do note that this contrasts with previous data (Cavaliere & Silvello, 2016). This indicates that process parameters and microstructure could have a profound impact on fatigue life. It has been noted (Kvedaras, Vilys, Ciuplys, & Ciuplys, 2006) that in steels, Cr coating can improve or significantly worsen the fatigue lifetime due to different microstructures produced in the coating.

These data indicate a critical need for an applicant to provide fatigue data from irradiated cladding that they have manufactured to support their safety analysis limits.

Table 6.10. Summary of unirradiated fatigue data for Cr-coated Zr cladding

Organization	Cladding	Test Description	Results
Czech Technical Institute (Sevecek, et al., 2018)	Cr coated Zry by cold spray	Fatigue cycling in air and in water between 300°C and 312°C	Fatigue failure observed significantly earlier in Cr coated samples (~10,000 cycles) than uncoated samples (100,000 to 500,000) cycles

6.4 Data Gaps and Performance Concerns

As noted at the beginning of this section, the data that are compiled here are intended to give the NRC staff expected performance of coated cladding as well as areas of concern that should be given additional scrutiny during the review of one of these concepts. The presence of data in any area does not indicate

that an applicant would not have to provide data from their specific coated cladding because it has been observed that coating processes and other processes can impact the performance of the cladding and the coatings.

The following summarizes at a high level the gaps in the publically available data and any concerns on performance that the current data have brought to light

6.4.1 Data Gaps

The following data needs are those where data is recommended for licensing, but currently none exists that would indicate what the performance of Cr-coated cladding would be.

Section 6.1 identified current and planned irradiation tests for Cr-coated Zr cladding and irradiation tests that would be recommended to collect in-reactor data for licensing. The following tests have been identified as not currently being planned, but recommended to collect for licensing.

- Irradiation creep tests
- Power ramp tests
- RIA tests.

Section 6.1 also identified data that is recommended for licensing that can be collected from current and planned irradiation tests through poolside examinations and post-irradiation examinations. These data have not yet been collected, but it is expected that they will be collected.

- Axial growth
- Oxidation rate
- Hydrogen pickup
- Rod bow
- Fission gas release
- Rod internal pressure and void volume.

Section 6.2 identified data that is recommended for licensing that can be collected on unirradiated cladding tubes. Those data that have not been collected include:

- Thermal properties (thermal expansion, thermal conductivity, heat capacity, and enthalpy)
- Fretting wear on grid components from hard coatings on rods
- Thermal limits such as CHF or DNB have not been evaluated (may not be necessary if surface finish is similar to uncoated rods).

Section 6.3 identified data that is recommended for licensing that can be collected on irradiated cladding tubes. Those data that have not been collected include:

- Irradiated mechanical properties (elastic modulus, yield stress, ultimate tensile strength, uniform elongation at temperatures relevant to normal operation, and RIA during the PCMI phase)

- Irradiated fatigue limits.

6.4.2 Performance Concerns

The following performance concerns for Cr-coated Zr have been identified based on the data presented in this section. Each is briefly discussed as follows.

Performance beyond eutectic. Data indicate localized melting in cladding tubes exposed to temperature greater than the Cr-Zr eutectic temperature of 1332°C. Although rod failure was not observed, additional scrutiny should be applied during the review to the impact of this localized melting if performance at or above this temperature is requested.

LOCA post quench ductility. LOCA post quench ductility may be improved for Cr-coated cladding as a function of time at temperature, but the current Zr-alloy cladding embrittlement limits of 1204°C and 17% ECR are likely not an appropriate embrittlement limit. Embrittlement has been observed in Cr-coated samples at 2-4% ECR. The cause of embrittlement in Cr-coated cladding is not currently known. A new limit is recommended.

Cracking of coating. Cracking of the Cr coatings has been observed at greater than 4% strain. This should be acceptable if current normal operation and AOO limits of around 1% cladding hoop strain are retained. However, for LOCA, cladding ballooning with large hoop strains (10%-50%) occur prior to high temperature oxidation. The cracking of the coating should be evaluated during the review if high temperature oxidation protection of the intact coating is credited for LOCA following ballooning to large strains.

Cladding fatigue life. Fatigue life could be profoundly impacted by the Cr-coating. Data indicate that Cr coatings can slightly increase or profoundly decrease the fatigue life of the substrate. A new fatigue limit is recommended for each Cr-coated cladding concepts based on data from irradiated cladding tubes that are manufactured in a prototypic manner.

7.0 Conclusions

Work toward commercialization and licensing of Cr-coated Zr cladding (including coatings of Cr-compounds) is well underway in the United States and elsewhere. This work is driving a need for regulatory preparedness by the NRC to receive licensing topical reports requesting approval of their specific concepts and the codes and methods that will be used to perform the safety analyses for fuel containing Cr-coated Zr cladding tubes.

Although it is the responsibility of the applicant to provide updated codes, methods, design limits, and the data to justify these, it is critical that NRC staff have an independent understanding of the existing data and potential damage mechanisms as well as the data that have previously been used to approve new cladding alloys.

This report provides an overview of the Cr-coated Zr concepts currently being developed in the U.S. and elsewhere (Section 2.0). Because the technique used to apply a coating has a large impact on the performance of that coating, an overview of the various coating technologies is provided (Section 3.0). Interaction between the Cr-coating and Zr-substrate is inevitable and therefore the Cr-Zr phase diagram is also provided (Section 4.0). The section includes discussion of formation of brittle phases, corrosion performance of these phases, and low temperature eutectics that could have a detrimental impact on cladding performance.

Section 5.0 provides a guide for NRC staff as they perform a review of an LTR, or LTR supplement related to the implementation of Cr-coated cladding. The section:

- Provides a list of cladding material property correlations that are typically needed to adequately model fuel system response and identifies data that are typically used to develop and justify these correlations.
- Discusses SAFDL limits in areas that are identified in Standard Review Plan Section 4.2, identifies data that are typically used to develop and justify these limits, and identifies potential new damage mechanisms that should be considered during the LTR review specifically for Cr-coated cladding with data that could be used to justify proposed limits.
- Discusses potential changes and data validation for existing codes and methodologies that may be implemented to perform safety analyses for Cr-coated cladding.

Section 5.0 also provides lists of tests that could be used to obtain material properties data (Table 5.1.), tests that could be used to establish design limits (Table 5.3), and tests that could be used to assess code performance (Table 5.4.) for Cr-coated Zr cladding.

Section 6.0 provides a summary of the literature review that was performed to identify the available data for Cr-coated Zr cladding relevant to licensing. These data include in-reactor tests and ex-reactor tests on both irradiated and unirradiated cladding. This literature review identifies data gaps in the following four categories. The specific gaps are listed in Section 6.4.1

- Irradiation tests not currently being planned but recommended to collect licensing data
- Data that has not yet been collected from currently known irradiation tests

- Data that is recommended to be collected on unirradiated cladding
- Data that is recommended to be collected on irradiated cladding.

Finally, the literature review identifies several performance concerns for Cr-coated Zr cladding. These concerns are listed below. These concerns may not manifest themselves in all concepts as various processing techniques can have a profound impact on cladding performance.

- Performance beyond Cr-Zr eutectic temperature of 1332°C
- LOCA post quench ductility. Current embrittlement limits of 1204°C and 17% ECR are likely not appropriate
- Cracking of coating during ballooning if high temperature oxidation protection is credited
- Cladding fatigue life may be significantly reduced by the application of the Cr-coating.

8.0 References

American Scociety of Mechanical Engineers. (2017). *Boiler and Pressure Vessel Code.* New York: American Scociety of Mechanical Engineers.

American Society for Metals. (1990). *ASM Handbook 10th Edition Metals Handbook.* Materials Park, OH: ASM International.

Anderson, V., & Van Nieuwenhove, R. (2016). *PIE on the coated fuel rods from IFA-774, HWR-1157.* Halden, Norway: OECD Halden Reactor Project.

Arias, D., & Abriata, J. (1986). *The Cr-Zr (Chromium-Zirconium) System. Bulletin of Alloy Phase Diagram.* American Society for Metals: 237-244.

Bischoff, J., Delafoy, C., Chaari, N., Vauglin, C., Buchanan, K., Barberis, P., . . . Nimishakavi, K. (2018). Cr-Coated Cladding Development at Framatome. *TopFuel 2018* (p. A0152). Prague, Czech Republic: European Nuclear Society.

Bischoff, J., Delafoy, C., Vauglin, C., Barberis, P., Roubeyrie, C., Perche, D., . . . Schweitzer, E. N. (2018). AREVA NP's enhanced accident-tolerant fuel developments: Focus on. *Nuclear Engineering and Technology*, 223-228.

Brachet, J., Dumerval, M., Lazaud-Chaillioux, V., Le Saux, M., Rouesne, E., Urvoy, S., . . . Pauillier, E. (2017). Behaviour of Enhanced Accident Tolerant Chromium Coated Zirconium Alloys Claddings. *Enlarged Halden Programme Group 2017* (p. F1.3). Lillehammer, Norway: OECD Halden Reactor Project.

Brachet, J., Guilbert, T., Le Saux, M., Rousselot, J., Nony, R., Toffolon-Masclet, C., . . . Pouillier, E. (2018). Behavior of Cr-Coated M5 Claddings during and After High Temperature Steam Oxidation from 800°C Uo to 1500°C (Loss-of-Coolant Accident & Design Extension Conditions). *TopFuel 2018* (p. A0100). Prague, Czech Republic: European Nuclear Society.

Brodnikovskii, N. P., Oryshich, I. V., Poryadchenko, N. E., Kuznetsova, T. L., Khmelyuk, N. D., & Rokitskaya, E. A. (2010). Resistance of Titanium - Chromium and Zirconium - Chromium Alloys to Air Oxidation. *Powder Metallurgy and Metal Ceramics*, 454-459.

Cavaliere, P., & Silvello, A. (2016). Fatigue behaviour of cold sprayed metals and alloys: critical review. *Surface Engineering*, 631-640.

Collier, J., & Thome, J. (1994). *Convective Boiling and Condensation, 3rd Ed.* Oxford, England: Oxford University Press.

Core, G. (2016). *Fuel Cycle Research and Development Accident Tolerant Fuels Series 1 (ATF-1) Irradiation Testing FY 2016 Status Report.* Idaho Falls: Idaho National Laboratory.

Cox, B. (2005). Some thoughts on the mechanisms of in-reactor corrosion of zirconium alloys. *Journal of Nuclear Materials*, 331-368.

Csontos, A. (2018). *Coated Cladding Gap Analysis, 3002014603.* Palo Alto, CA: EPRI.

Delafoy, C., Bischoff, J., Larocque, J., Attal, P., Gerken, L., & Nimishakavi, K. (2018). Benefits of Framatome's E-ATF Evolutionary Solution: Cr-Coated Cladding with Cr2O3-Doped Fuel. *TopFuel 2018* (p. A0149). Prague, Czech Republic: European Nuclear Society.

Dumerval, M., Houmaire, Q., Brachet, J., Palancher, H., Bischoff, J., & Pouillier, E. (2018). Behavior of Chromium Coated M5 Claddings upon Thermal Ramp Tests under Internal Pressure (Loss-of-Coolant Accident Conditions). *TopFuel 2018* (p. A0102). Prague, Czech Republic: European Nuclear Society.

Fauchais, P., Heberlein, J., & Boulos, M. (2014). *Thermal Spray Fundamentals: From Powder to Part.* Boston, MA: Springer.

Flanagan, M., Askeljung, P., & Puranen, A. (2013). *Post-TEst Examination Results from Integral, High-Burnup, Fueled LOCA Tests at Studsvik Nuclear Laboratory, NUREG-2160.* Washington D.C.: U.S. Nuclear Regulatory Commission.

Garde, A., Pati, S., Krammen, A., Smith, G., & Endter, R. (1993). Corrosion Behavior of Zircaloy-4 Cladding with Varying Tin Content in Hight-Temperature Pressurized Water Reactors. *Zirconium in the Nuclear Industry, Tenth International Symposium*, 760-778.

Gärtner, F., Stoltenhoff, T., Schmidt, T., & Kreye, H. (2006). The Cold spray process and its potential for industrial applications. *Journal of Thermal Spray Technology*, 223-232.

Geelhood, K., & Luscher, W. (2015). *FRAPCON-4.0: Integral Assessment, PNNL-19418, Vol.2 Rev.2.* Richland, WA: Pacific Northwest National Laboratory.

Geelhood, K., Beyer, C., & Cunningham, M. (2004). Modifications to FRAPTRAN to Predict Fuel Rod Failures Due to PCMI during RIA-Type Accidents. *2004 International Meeting on LWR Fuel Performance* (p. 1097). Orlando, FL: American Nuclear Society.

Geelhood, K., Beyer, C., & Luscher, W. (2008). *PNNL Stress/Strain Correlation for Zircaloy. PNNL-17700.* Richland, WA: Pacific Northwest National Laboratory.

Geelhood, K., Luscher, W., Beyer, C., Senor, D., Cunningham, M., Lanning, D., & A. H. (2009). *Predictive Bias and Sensitivity in NRC Fuel Perofrmance Codes, NUREG/CR-7001, PNNL-17644.* Washington DC: U.S. Nuclear Regulatory Commission.

Geelhood, K., Luscher, W., Cuta, J., & Porter, I. (2016). *FRAPTRAN-2.0: A Computer Code for the Transient Analysis of Oxide Fuel Rods, PNNL-19400, Vol.1 Rev.2.* Richland, WA: Pacific Northwest National Laboratory.

Geelhood, K., Luscher, W., Raynaud, P., & I.E., P. (2015). *FRAPCON-4.0: A Computer Code for the Calculation of Steady-State, Thermal-Mechanical Behavior of Oxide Fuel Rods for High Burnup, PNNL-19418, Vol.1 Rev.2.* Richland, WA: Pacific Northwest National Laboratory.

Girardin, G., Meier, R., Jatuff, F., Bischof, J., Delafoy, C., & Schweitzer, E. (2018). Inspection Capabilities and In-Pile Exerience with Innovative and Enhanced Accident Tolerant Fuel Materials at KKG. *TopFuel 2018* (p. A0178). Prague, Czech Republic: European Nuclear Society.

Grainger, S. (1998). *Engineering Coatings: design Application. Second Edition.* Cambridge, England: Abington Publishing.

Harp, J. M., & Cappia, F. (2019). Accident Tolerant Fuels (ATF-1) Irradiation Tests: overview of the ongoing post-irradiation examinations. *Transactions of the American Nuclear Society* (p. 1602). Philadelphia, Pennsylvania: American Nuclear Society.

Idaho National Laboratory. (2018). *Report to NEAC Nuclear Technology R&D Subcommittee Meeting of May 7, 2018.* Idaho Fall, ID: Idaho National Laboratory.

Kandlikar, S. (2001). A theoretical model to predict pool boiling CHF incorporating effects of contact angle and orientation. *Journal of Heat Transfer*, 1071-1079.

Kim, H.-G., Kim, I.-H., Jung, Y.-I., Park, D.-J., Park, J.-Y., & Koo, Y.-H. (2015). Adhesion property and high-temperature oxidation behavior of Cr-coated Zircaloy-4 cladding tube prepared by 3D laser coating. *Journal of Nuclear Materials*, 531-539.

Kim, H.-G., Yang, J.-H., Kim, W.-J., & Koo, Y.-H. (2016). Development Status of Accident-tolerant Fuel for Light Water Reactors in Korea. *Nuclear Engineering and Technology*, 1-15.

Kim, H.-G., Yang, J.-H., Koo, Y.-H., Kim, J., Shin, H., Yoo, J., & Mok, Y.-K. (2018). Overview of Accident Tolerant Fuel Development for LWRs. *TopFuel 2018* (p. A0036). Prague, Czech Republic: European Nuclear Society.

Krejci, J., Sevecek, M., Kabatova, J., Manoch, F., Koci, J., Cvrcek, L., . . . Namburi, H. (2018). Experimental Behavior of Chromium-Based Coatings. *TopFuel 2018* (p. A0233). Prague, Czech Republic: European Nuclear Society.

Kvedaras, V., Vilys, J., Ciuplys, V., & Ciuplys, A. (2006). Fatigue Strength of Chromium-Plated Steel. *Materials Science*, 16-18.

Limback, M., & Andersson, T. (1996). A Model for Analysis of the Effect of Final Annealing on the Inand Out-of-Reactor Creep Behavior of Zircaloy Cladding. *Zirconium in the Nuclear Industry: Eleventh International Symposium, ASTM STP 1295*, 448-468.

Lin, Y., Faucett, R., Desilva, S., Lutz, D., Yilmaz, M., Davis, P., . . . Satterlee, N. (2018). Path Toward Industrialization of Enhanced Accident Tolernat Fuel. *TopFuel 2018* (p. A0141). Prague, Czech Republic: European Nuclear Society.

Liu, T., Zue, J. L., Li, L., Guo, D., Zhang, Q., & Xu, D. (2018). The research on Accident Tolerant Fuel in CGN. *TopFuel 2018* (p. A0244). Prague, Czech Republic: European Nuclear Society.

Luscher, W., Geelhood, K., & Porter, I. (2015). *Material Property Correlations: Comparisons between FRAPCON-4.0, FRAPTRAN-2.0, and MATPRO, PNNL-19417 Rev.2.* Richland, WA: Pacific Northwest National Laboratory.

Michau, A., Maury, F., Schuster, F., Lomello, F., Brachet, J.-C., Rouesne, E., . . . Pons, M. (2018). High-temperature oxidation resistance of chromium-based coatings deposited by DLI-MOCVD for enhanced protection of the inner surface of long tubes. *Surface & Coatings Technology*, 1048-1057.

O'Donnell, W., & Langer, B. (1964). Fatigue Design Basis for Zircaloy Components. *Nuclear Science and Engineering*, 1-12.

OECD, NEA. (2018). *State-of-the-Art Report on Light Water Reactor Accident-Tolerant Fuels.* Paris, France: Nuclear Energy Agency.

Oelrich, R., Ray, S., Karoutas, Z., Xu, P., Romero, J., Shah, H., . . . Boylan, F. (2018). Overview of Westinghouse Lead Accident Tolerant Fuel Program. *TopFuel 2018* (p. A0151). Prague, Czech Republic: European Nuclear Society.

Oelrick, R., Xu, P., Lahoda, E., & Deck, C. (2018). Update on Westinghouse EnCore® Accident Tolerant Fuel Program. *Transactions of the American Nuclear Society, Vol. 118* (p. 1311). Philadelphia, Pennsylvania: American Nuclear Society.

O'Hanley, H., Coyle, C., Buongiorno, J. M., Hu, L., Rubner, M., & Cohen, R. (2013). *Separate effects of surface roughness, wettability, and porosity on the boiling critical heat flux.*

Ohta, T., Nakagawa, Y., Kaneno, Y., & Kim, W.-Y. (2003). Microstructures and mechanical properties of NbCr 2 and ZrCr 2 Laves phase alloys prepared by powder metallurgy. *Journal of Materials Science* , 657-665.

Oryshich, I., Poryadchenko, N., & Brodnikovskii, N. (2004). High-Temperature Oxidation of Intermetallics formed by Group IV transition metals with chromium. *Powder Metallurgy and Metal Ceramics*, 497-503.

Park, D., Kim, H., Jung, Y., Park, J., Yang, J., & Koo, Y. (2016). Behavior of an improved Zr fuel cladding with oxidation resistant coating under loss-of-coolant accident conditions. *Journal of Nuclear Materials*, 75-82.

Pierson, H. (1999). *Handbook of Chemical Vapor Deposition: Principles, Technology and Applications, Second Editions.* Norcich, New York: William Andrew Publishing, LLC.

Powers, D., & Meyer, R. (1980). *Cladding Swelling and Rupture Models for LOCA Analysis, NUREG-0630.* Washington DC: U.S. Nuclear Regulatory Commission.

Sabol, G., Comstock, R., Weiner, R., Larouere, P., & Stanutz, R. (1993). In-Reactor Corrosion Performance of ZIRLO and Zircaloy4. *Zirconium in the Nuclear Industry, Tenth International Symposium*, 724-744.

Sevecek, M., Gurgen, A., Seshadri, A., Che, Y., Wagih, M., Phillips, B., . . . Shirvan, K. (2018). Development of Cr cold sprayecoated fuel cladding with enhanced accident tolerance. *Nuclear Engineering and Technology*, 229-236.

Sevecek, M., Krejci, J., Shahin, M., Petrik, J., Ballinger, R., & Shirvan, K. (2018). Fatigue Behavior of Cold Spray-Coated Accident Tolerant Cladding. *TopFuel 2018* (p. A0126). Prague, Czech Republic: European Nuclear Society.

Shaffer, C., Leonard, M., Letellier, B., Rao, D., Maji, A., Howe, K., . . . Madrid, J. (2005). *GSI-191: Experimental Studies of Loss-of-Coolant-Accident-Generated Debris Accumulation and Head Loss with Emphasis on the Effects of Calcium Silicate Insulation, NUREG/CR-6874, LA-UR-04-1227.* Los Alamos, NM: Los Alamos National Laboratory.

Shah, H., Romero, J., Xu, P., Oelrich, R., Walter, J., Wright, J., & Gassmann, W. (2018). Westinghouse-Exelon EnCore® Fuel Lead Test Rod (LTR) Program including Coated cladding Development and Advanced Pellets. *TopFuel 2018* (p. A0145). Prague, Czech Republic: European Nuclear Society.

Shahin, M., Petrik, J., Seshadri, A., Phillips, B., & Shirvan, K. (2018). Experimental Investigation of Cold-Spray Chromium Cladding. *TopFuel 2018* (p. A0193). Prague, Czech Republic: European Nuclear Society.

Sweeney, W., & Batt, A. (1964). Electron Proble and X-ray Diffraction Measurements of Intermediate Phases in Zr Diffused with Cr, Fe, Ni, Cu and Mo. *Journal of Nuclear Materials*, 87-91.

Szoke, R., & Bennett, P. (2017). Initial REsults from the Accident Tolerant Cladding Test IFA-796. *Enlarged Halden Programme Group 2017* (p. F1.1). Lillehammer, Norway: OECD Halden Reactor Project.

Takata, Y., Hidaka, S., Masuda, M., & Ito, T. (2003). Pooling boiling on a superhydrophilic surface. *Journal of Energy Research*, 111-119.

Terrani, K. (2018). Accident tolerant fuel cladding development: Promise, status, and challenges. *Journal of Nuclear Materials*, 13-30.

US Nuclear Regulatory Commission. (2007). *Standard Review Plan Section 4.2 Fuel System Design, Revision 3, NUREG-0800* . Washington DC: US Nuclear Regulatory Commission.

US Nuclear Regulatory Commission. (2017). *Title 10 Code of Federal Regulations Part 50.45 Acceptance Criteria for Emergency Core Cooling Systems for Light-Water Nuclear Power Reactors.* Washington DC: US Nuclear Regulatory Commission.

Van Nieuwenhove, R. (2014). *IFA-774: The first in-pile test with coated fuel rods, HWR-1106.* Halden, Norway: OECD Halden Reactor Project.

Wang, Y., Zhou, W., Wen, Q., Ruan, X., Luo, F., Bai, G., . . . Li, R. (2018). Behavior of plasma sprayed Cr coatings and FeCrAl coatings on Zr fuel. *Surface & Coatings Technology*, 141-148.

Weatherford, R. (1963). *Nucleate boiling characteristics and critical heat flux occurrence in sub-cooled axial flow water systems ANL 6675.* Argonne, IL: Argonne National Laboratory.

Wenxin, X., & Shihao, Y. (2001). *Reaction Diffusion in Chromium-Zircaloy-2 System, CNIC-01562.* Chengdu: Nuclear Power Institute of China.

Xu, P., Wright, J., Lahoda, E., Romero, J., Middleburgh, S., Shah, H., . . . Oelrich, R. (2017). Westinghouse Accident Tolerant Fuel Materials. *Enlarged Halden Program Group* (p. F1.4). Lillehammer, Norway: OECD Halden Reactor Project.

Zhao, Z., Kunii, D., Abe, T., Yang, H., Shen, J., & Shinohara, Y. (2017). A comparative study of hydride-induced embrittlement of Zircaloy-4 fuel cladding tubes in the longitudinal and hoop directions. *Journal of Nuclear Science and Technology* , 490-499.

Pacific Northwest
NATIONAL LABORATORY

www.pnnl.gov

902 Battelle Boulevard
P.O. Box 999
Richland, WA 99352
1-888-375-PNNL (7665)

U.S. DEPARTMENT OF
ENERGY